Genome Wide Variant Analysis of Simplex Autism Families with an Integrative Clinical-Bioinformatics Pipeline

Laura T. Jiménez-Barrón[1,5], Jason A. O'Rawe[1,2], Yiyang Wu[1,2], Margaret Yoon[1] , Han Fang[1], Iossifov Ivan[1], Gholson J. Lyon[1,2,4,*]

1) Stanley Institute for Cognitive Genomics, Cold Spring Harbor Laboratory, NY, USA;
2) Stony Brook University, Stony Brook, NY, USA;
3) Department of Pediatrics, University of Utah, Salt Lake City, UT, USA;
4) Utah Foundation for Biomedical Research, Salt Lake City, UT, USA;
5) Centro de Ciencias Genomicas, Universidad Nacional Autonoma de Mexico, Cuernavaca, Morelos, MX

* Corresponding author e-mail:
Gholson J. Lyon: gholsonjlyon@gmail.com

Other author emails:
Laura T. Jimenez Barrón: laurajb@lcg.unam.mx
Jason A. O'Rawe: jazon33y@gmail.com
Yiyang Wu: wuyiyang.cshl@gmail.com
Margaret Yoon: margopolo9590@gmail.com
Han Fang: hfang@cshl.edu
Ivan Iossifov: iossifov@cshl.edu

Short running title: Genome Wide Variant Analysis of ASD families

Abstract

Autism spectrum disorders (ASD) are a group of developmental disabilities that affect social interaction, communication and are characterized by repetitive behaviors. There is now a large body of evidence that suggests a complex role of genetics in ASD, in which many different loci are involved. Although many current population scale genomic studies have been demonstrably fruitful, these studies generally focus on analyzing a limited part of the genome or use a limited set of bioinformatics tools. These limitations preclude the analysis of genome-wide perturbations that may contribute to the development and severity of ASD-related phenotypes. To overcome these limitations, we have developed and utilized an integrative clinical and bioinformatics pipeline for generating a more complete and reliable set of genomic variants for downstream analyses. Our study focuses on the analysis of three simplex autism families consisting of one affected child, unaffected parents, and one unaffected sibling. All members were clinically evaluated and widely phenotyped. Genotyping arrays and whole genome sequencing were performed on each member, and the resulting sequencing data were analyzed using a variety of available bioinformatics tools. We searched for rare variants of putative functional impact that were found to be segregating according to de-novo, autosomal recessive, x-linked, mitochondrial and compound heterozygote transmission models. The resulting candidate variants included three small heterozygous CNVs, a rare heterozygous *de novo* nonsense mutation in *MYBBP1A* located within exon 1, and a novel *de novo* missense variant in *LAMB3*. Our work demonstrates how more comprehensive analyses that include rich clinical data and whole genome sequencing data can generate reliable results for use in downstream investigations. We are moving to implement our framework for the analysis and study of larger cohorts of families, where statistical rigor can accompany genetic findings.

Introduction

In 2010, the Center for Disease Control and Prevention (CDC) found that 1 in 68 eight-year-olds were diagnosed with ASD in the United States across 11 surveyed locations [1], with males being diagnosed 5 times more often than females [2-4]. Although the prevalence of ASD across different ethnicities, countries and social groups appears to be heavily influenced by methodological variables during diagnosis [5], it is clear that ASD is an emerging public health concern. Studies contributing to a better understanding of its causes and mechanisms promise to enable more precise diagnoses [6, 7], more effective treatments, and preventative care.

There is a vast and consistent amount of evidence suggesting a complex role of genetics in ASD [2, 6-12], in which many different loci are involved, but a general understanding of what causes ASD on a molecular and physiological level has not yet emerged. This question is broadly studied [2, 13-15], but the diversity of approaches used towards answering it has not led to broad conclusions about its etiology. Indeed, there is a large collection of putative disease contributing variants found in ASD diagnosed people, yet only a small fraction of these variants are reliably detected in small subpopulations of ASD patients [6, 7, 16, 17], leaving most ASD cases of undetermined etiology. The lack of generality in these findings may be attributed to many factors, including the phenotypic heterogeneity of the disease [8], the need for larger sample sizes for statistical studies [13], and to variability in the methodology used to analyze ASD-related data.

Currently, many ASD studies focus on the analysis of microarray and/or exome sequencing data for understanding the etiological contributions to and mechanisms of ASD [4, 9, 13]. These analyses are generally applied to large cohorts, such as those from the Simons Simplex Collection [4, 18], which consists of families with a single affected child, unaffected parents and at least one unaffected sibling. Those studies generally use and analyze only one of the high throughput sequencing technologies mentioned above, with varying levels of sequence coverage for WES or genotyping markers (for genotyping microarrays). Furthermore, these studies use only one or a few analysis tools for detecting sequence variations, which can result in a loss of information in situations where one tool performs poorly. Although these approaches have led to significant genetic discovery [4, 13], they are likely to miss-call or simply miss true and disease-relevant genetic variation. Some tools may perform better on just one or a few areas of the genome, and their performance may also differ depending on dataset-specific characteristics. To address this problem, we describe an integrative clinical and bioinformatics pipeline that makes use of a variety of analysis tools and orthogonal high throughput sequencing technologies to obtain a more complete and reliable set of candidate ASD-variants for validation and downstream functional analysis.

Results

This study consisted of the clinical recruitment of three Simplex Autism Families **(Figure 1)** for phenotyping and whole genome studies. Human sequence variation spans a variety of genomic scales, ranging from single nucleotide to megabase and even whole chromosome differences. Due to the variety of scales and mechanisms that can lead to variation in human sequence between individuals and populations, a variety of algorithms are needed in order to extract genomic signatures at all scales and that

represent a wide variety of variant types. A variety of variant discovery algorithms and procedures were used during the course of this study, each designed to detect different classes of human sequence variants (**Figure 2**).

Simon's Simplex Collection Phenotypic evaluation results

Body Mass Index (BMI), head circumference, height and weight were measured for both probands stemming from the two Simons Simplex Collection (SSC) families studied here (**Table 1**). General IQ (intellectual quotient) as well as verbal IQ and non-verbal IQ were measured for both SSC probands. Table 2 details the evaluative instruments used for each SSC family. Similar body and cognitive measurements were not available for the third K22 proband **(Table 1**), although ancestral background was recorded for all three probands.

Concordance between variant detection algorithms

In this section, we explore detection reliability by measuring concordance among algorithm results across all sequenced individuals. Single nucleotide variants, small insertions or deletions and the detection of *de novo* variants of either class were compared across algorithms applied to raw whole genome sequencing (WGS) data.

Single nucleotide variants (SNVs) and small insertions or deletions (INDELs)
GATK (the Genome Analysis Toolkit) and Freebayes are algorithms that detect both SNVs and INDELs across the entire sequenced genome; as such, we report here the concordance between these two algorithms in detecting SNVs and INDELs. The observed mean concordance between GATK and Freebayes was 79.3% and 56.6% for filtered SNV and INDEL calls, respectively. After filtering for high quality variants according to each algorithm's recommendation (see methods), concordance between the algorithms increases by 5.7% and 5.4% for SNVs and INDELs respectively. Table 3 summarizes the mean per person number of variants called by each algorithm.

De-novo unique SNVs
The mean number of unfiltered unique *de novo* SNVs (not shared by siblings) detected by the Multinomial Analyzer, Freebayes and GATK was 65,572, 76,920 and 40,873 respectively. The Multinomial Analyzer is an algorithm specifically designed to detect *de novo* SNVs, where as additional steps were taken to obtain a list of putative *de novo* variants using Freebayes and GATK. After filtering variants based on each algorithm's recommendations (refer to the Methods section for details pertaining to the filtering procedures), the mean number of variants detected by each caller dropped to 1,692, 24,982 and 31,831 for the Multinomial Analyzer, Freebayes and GATK, respectively. The concordance between the 3 algorithms was generally low, with Freebayes and GATK agreeing on 12.4% of their detected variants, and all three agreeing on less than one percent of the total filtered call-set, 0.113%. It is important to note that the low concordance between the Multinomial Analyzer and the other algorithms is influenced by the fact that its filtering step considers a '*de novo* score', which is something that the other algorithms do not use for filtering purposes. Thus, the large difference in overall call rate makes a comparison of the mean overlapping calls somewhat uninformative, as the intersection between all three can only be as large as the smallest set. It is for this reason that the union of the three algorithms was considered during downstream prioritization steps, rather than the intersection.

De-novo unique INDELs

De-novo INDELs from GATK, Freebayes and Scalpel were also compared. The mean number of *de novo* INDELs detected by GATK, Freebayes and Scalpel per proband before filtering was 52,631, 55,505 and 128 respectively, and after filtering based on each algorithm's recommendations, this number dropped to 42,425, 37,210 and 70. The concordance between the three algorithms was, again, low. Freebayes and GATK agreed on 10.7% of the total call set, and all three callers agreed on only one variant and only within the subset of a single family (i.e., there was only one instance in which all three callers found the same variant). One should keep in mind that the filtering criteria and size of call sets are very different across these three callers, so our a-priori expectation is that a low number of calls will be within the intersection of all three.

Variant classification and prioritization for SNVs and INDELs

After obtaining high quality call sets from the union of filtered variants from all algorithms and categorizing them according to different disease models, the number of variants was still too large to proceed to more detailed literature searches and putative functional interpretations. Filtering variants by CADD score > 20 and MAF < 0.01 from 1000 genomes reduced the number of variants for consideration dramatically (**Table 4**) and the number of compound heterozygous mutations was reduced to zero. However, variants segregating according to the compound heterozygous model are not necessarily expected to be deleterious on their own, but may be deleterious in combination with other variants in the same gene on the same, or different, chromosome.

To narrow the list of possible disease contributing variants, each call set was annotated and filtered using various criteria and scores described in the Methods section. Out of the resulting prioritized variants, an average of 101 per family were localized to intra or intergenic regions (**Supp. Table 1**) and only three were located within a gene, one of which was found to be common in the SSC controls. Thus, by these filtering criteria, two exonic variants were considered as potentially contributing to the disease (**Table 5**). The genic variants are described below.

MYBBP1A stop gain variant

A *de novo* heterozygous nonsense mutation was found on the first exon of *MYBBP1A* (chr17: 4,442,191-4,458,926) in pedigree K21 **(Figure 3)**. This mutation is located at chr17:4458481, it is a G->A substitution and is annotated as being highly deleterious with a CADD score of 40, which corresponds to being within the top 0.01% of all possible SNVs in terms of its deleteriousness. The variant was not found in DBsnp Human Build 142 [19], the exome variant server [http://evs.gs.washington.edu/EVS/] or in any other person in the Simon's Simplex Collection database. One proband from the SSC was found to have a *de novo* missense G->T substitution in the same gene located at chr17: 4444853 causing an Arg->Ser change. Only one person out of 71,164 unrelated individuals from the Exome Aggregated Consortium [http://exac.broadinstitute.org] is reported to have this exact same mutation, indicating that this is a very rare variant. As the phenotype of this person in the ExAC database with the mutation is unknown, and also given that there are people with neuropsychiatric conditions in ExAC, no conclusions can be made from this alone. Sanger sequencing validated this mutation (**Supp. Fig. 1**).

LAMB3 missense variant

The second *de novo* mutation detected in the study was found in the SSC_1 pedigree, this time a missense mutation located at chr1:209823359 on *LAMB3* **(Figure 4)**. Although this mutation was reported in a previous study [13], it was not found in any other person contained within the SSC database and it was not found in any of the other interrogated databases, the exome variant server, or the ExAC database, making it an ultra rare mutation.

Variant classification and prioritization for copy number variations

On average, 1500 unfiltered deletions and 450 unfiltered duplications were detected by ERDS applied to the WGS data (see Methods) for each person in the study. After filtering (see Methods), 150 deletions and 170 duplications were found on average per person. The number of calls obtained with PennCNV was highly variable, with a mean of 60 unfiltered duplications (sd=38) and a mean of 80 unfiltered deletions (sd=29) being detected. After filtering the variants, only 5% and 20% of all duplications deletions were retained, respectively. After annotating, none of the remaining CNVs were identified as pathogenic. However, we detected three CNVs **(Figure 5-7)** whose coordinates **(Table 6)** are embedded within larger CNVs that have been associated with cognitive disease. These CNVs were not found in any other unaffected family member. Two out of the three CNVs were found in pedigree K21, however only the ERDS algorithm detected them. As described in the Methods section, PennCNV uses the Log R Ratio (LRR) and B Allele Frequencies (BAF) to detect a CNV. Different numbers of copies have different clustering patterns for the LRR and BAF values when plotted. In pedigree K21 **(Figure 5,6)**, both the LRR and BAF are not properly clustered, suggesting, in this case, that these CNVs were not detected by PennCNV but were detected by ERDS as true positives, due to the properties of the microarray dataset for this family.

CGH microarray sequencing and analysis applied to the proband and his mother revealed the presence of a maternally inherited duplication spanning several genes (chrX:69074860-69512431). The duplication completely overlapped *OTUD6A*, *IGBP1*, *DGAT2L6*, *AWAT1*, *AWAT2*, *P2RY4*, *KIF4A*, *ARR3*, *GDPD2*, *RAB41*, *PDZD11* and partially overlapped *EDA*, *DLG3*, and *DLG3*. However, WGS-based CNV analyses revealed that the CNV was also present in the healthy sibling **(Supp. Fig. 6a)**. PennCNV, which was applied to additional Illumina microarray data, did not accurately call the breakpoints for this CNV in any of the three individuals where it was initially detected (mother, proband, sibling), although its presence was clear from manual inspection of the microarray data (see **Supp. Fig. 6b)**.

FMR1 test

Fragile X testing resulted in a normal number of CGG tri-nucleotide repeats for the K21 proband. Analysis of WGS data from all probands did not show any significant difference in CGG repeat content from the reference genome **(Supp. Fig. 2-5)**. Traditional clinical Fragile X testing does not include sequencing *FMR1*, thus potentially missing other mutations that can contribute to the development of Fragile X syndrome [20-25]. Although the probands in this study did not present any of the common phenotypic features of Fragile X, a profile of all the CGG repeats present in every person was generated using WGS data and these profiles compared to the reference sequence **(Supp. Fig 3-5).** No point mutations reported in the literature as contributing to Fragile X were found in any of the probands [24].

Reproducibility of previous exome studies

As different approaches were taken to retrieve the variants for each proband, it was of interest to know if all of the SSC proband's variants detected in the previous exome study, listed in **Table 7** [13], were also detected by the methods used here. In cases where a variant was missed, this type of analysis will enable us to identify which step of the analysis pipeline might be responsible. Out of the three previously reported variants, which belong only to one family (SSC_2) only one was included in the final list of variants with this pipeline. Two of the three were lost by GATK after the initial filtering step, but they were still included in the downstream analysis because Freebayes and the Multinomial Analyzer still detected and retained them in their call sets. However, they were ultimately discarded after the CAAD score prioritization step, as they were not included in the top 1% most deleterious variants (<20 CAAD score). No variants were found in the SSC_1 family, and none of the variants reported in **Table 7** were found in SSC_1 or K21.

Discussion

Concordance between algorithms

It is known that different algorithms are better at calling particular types of variants, each capable of detecting variants others cannot, and that they all usually agree on a subset of reliably called regions [26]. For this reason, the results of different algorithms were integrated, and instead of considering only the intersection of variants common to all algorithms, the union of all variant sets was obtained. This enabled the retention of variants that would have otherwise been excluded due to performing intersections with call sets, as only variants agreeing among all callers would have been retained. Indeed, one of the steps in which many variants are lost is during the initial filtering steps applied to each algorithm's raw call set, at which point one can to decide how stringent the filter should be. Even recommended filtering parameters resulted in a detectable level of false negatives, i.e. true variants excluded from the final call set, despite these parameters being optimized for both sensitivity and specificity. Because the probands included in our study had already been part of previously reported targeted sequencing experiments, we were able to leverage available validation data to identify which informatics steps would have resulted in false negative calls. In our study, we found that for the GATK HC call set, not all of the previously validated calls [13] passed the first initial recommended filtering steps.

To measure concordance between the different variant calling algorithms used here, we considered variants in agreement if they match in terms of the genomic positions where each algorithm made a call. Due to large differences in INDEL calling and reporting, the same INDEL can sometimes be reported differently [27]. For this reason, the reference and alternative fields were not included in the analysis of concordance between the different INDEL callers. Another reason for comparing callers in this way is based on the large differences seen in multiallelic calls reported by GATK HC (~30K) and Freebayes (~70K). This non-standard way of reporting indels has made the comparison between algorithms particularly difficult, thus, the comparisons performed in this study are approximate. These issues underscore the importance of carefully integrating sets of variants from different variant callers, as simple intersections can dramatically reduce the number of true positives even if all callers detect them, as their representations may be slightly different between the different callers. New tools that standardize discordant

variant reporting into a unified schema have been developed [28], and we expect that these tools will aid the in the more precise comparison and use of variants stemming from different callers.

Microarray vs. WGS data for detecting CNVs

Microarray data provides researches with a cheap yet powerful way of detecting CNVs; however, depending on the particular technology used as well as the algorithms used to analyze the generated data, the results can vary widely. Sparse markers in some genomic regions makes it difficult to define accurate breakpoints of detected CNVs, something that is less difficult with CNVs detected from WGS data. This is due, in part, to the fact that WGS data is more uniform; having an average coverage of reads which is less variable across the genome. For this study we had both types of data for one of the quads, making it possible to call variants from both sources and compare the results. We found a large degree of variation in terms of the number of CNVs detected per person and also between the two detection methods used (that is, WGS based and DNA microarray based methods). The genome-wide sensitivity of CNV detection using WGS is higher, due to the fact that array based methods do not densely cover the entire human genome with markers. We found that having data from these orthogonal technologies was useful in including or excluding true or false positive calls, as each should show some evidence of a CNV, if one does exist. Thus, in regions where both technologies had enough data to detect CNVs, discordant calls could be easily resolved by comparing the data profiles between the two.

Prioritization methods

Variant prioritization is another potentially delicate and important step in finding candidate disease contributing variants. One could detect all true variants from WGS analysis yet still discount biologically important variants if the pertinent annotations are not used correctly. When filtering based on annotations that are numerically scaled, filtering threshold values should generally be strict enough to result in a small number of variants in which functional studies are feasible, without letting any biologically important variant go unconsidered. Obtaining this variant set from a single annotation or score is currently not possible, as each individually lacks the power to filter to a small and manageable set, which could otherwise be obtained by using multiple annotations for threshold-based filtering. For these reasons, several tools and annotations were combined in order to make sure that the results were robust and not due to systematic errors from one prioritization framework. Although two different frameworks were used, they were only slightly different in their results, likely due to the fact that the VEP-GEMINI toolset has more annotations to determine if a variant is deleterious than does the in-house toolset. Unfortunately, using these two methods, we were unable to find a single candidate SNV or INDEL variant for the SSC_2 pedigree. One alternative would be to use other prioritizing methods, such as the Variant Annotation, Analysis, and Search Tool (VAAST), which employs an aggregative variant association test that combines both amino acid substitution (AAS) and allele frequencies and incorporates information about phylogenetic conservation [29]. As human variation not only includes small variations (SNVs and INDELs) and CNVs, but also structural variants and repeats, other software tools have to be used on these WGS data to explore other sources of variation that might contribute to disease.

Candidate variants

After initial filtering, variant prioritization and segregation analyses, we found two *de novo* missense variants that were annotated as being highly deleterious (as defined by a CADD score of greater than 20) and rare on the population level (with population allele frequencies less than 0.01). The first variant was found in the proband of the SSC_2 pedigree and it is a stop gain variant in *MYBBP1A*, and the second is a missense in *LAMB3* found in the proband from the K21 pedigree.

Stop gain in MYBBP1A

MYBBP1A codes for a nucleolar transcriptional regulator that was first identified by its ability to bind specifically to the Myb proto-oncogene protein [30]. The encoded protein is thought to play a role in many cellular processes including response to nucleolar stress, tumor suppression and the synthesis of ribosomal DNA, and many cancers have been previously associated with MYBBP1A including brain glioma [31]. According to UniProt [32], it may activate or repress transcription via interactions with sequence specific DNA-binding proteins and repression may be mediated at least in part by histone deacetylase activity. It has been shown that its down-regulation induces apoptosis and mitotic anomalies in mouse embryonic stem cells, embryonic fibroblasts and human HeLa cells [33]. The known information about MYBBP1A does not make any obvious connection to ASD, however it has not been possible to create a homozygous knock out mouse for MYBBP1A and this is thought to happen as it is essential for early mouse development prior to blastocyst formation [33]. In this study the mutation found in this gene is heterozygous and although healthy heterozygous knock out mice have been reported, it is not clear if those mice had similar any behavioral phenotypes related to autism; further studies are needed before any conclusions about the relevance of this variant in the etiology ASD can be made.

LAMB3

LAMB3 codes for a beta subunit laminin that belongs to a family of basement membrane proteins. Together with an alpha and a gamma subunit, LAMB3 forms laminin-5. It's known that mutations in this gene can cause Autosomal-dominant Amelogenesis Imperfecta [34], epidermolysis bullosa junctional Herlitz type, and generalized atrophic benign epidermolysis bullosa, diseases that are characterized by blistering of the skin [35]. According to UniProt [31], its function is to bind to cells via a high affinity receptor, laminin is thought to mediate the attachment, migration and organization of cells into tissues during embryonic development by interacting with other extracellular matrix components. Again, the known diseases associated with this gene do not have an obvious link to autism, but its participation during embryonic development makes it an interesting candidate for further functional studies.

Although we found CNVs and SNVs that fit the filtering and annotation criteria described in the Methods section, there is no obvious connection between any of them and ASD, so they should be carefully considered only as possible disease contributing variants that are in need of further functional analysis. In addition, we did not have the statistical power of a larger study to be able to associate our variants as casual factors in the development of autism, and so our results are restricted to interpretation in the context of the three families studied here.

Conclusions

Although a subset of ASD cases are now better understood, with their genetic contributions becoming more clear [2, 6, 8, 10, 13, 16, 17], the large degree of phenotypic heterogeneity in ASD leaves the vast majority of cases still poorly understood. Larger studies have focused on a subset of variant types, but here we have obtained a broader and more complete view of all the different types of genomic variation that could be contributing to the ASD phenotypes observed in this study. By combining different algorithms and variant prioritization methods, we were able to use the strengths of each and compensate for the different weaknesses by integrating their results in one computational framework.

There has been special interest in knowing to what extent *de novo* mutations are responsible for ASD cases [13]. In this study, four different variant detection algorithms and three different prioritization methods were used to detect *de novo* variants. This allowed us to improve detection sensitivity and to reduce the false negative rate. We also searched for variants segregating according to other disease transmission models, including autosomal recessive, X-linked, mitochondrial and compound heterozygote. As expected, the number of possible disease-contributing variants detected from each model varies widely (**Table 4**).

As sequencing technologies improve in accuracy and their operational costs decrease, large sequencing studies including thousands of people at higher sequencing depths are becoming more common. As such, it is useful and perhaps even necessary to design studies that search for and aim to detect all known variant types and to not just focus on a small subset. We suspect that such studies would, in general, obtain more biologically relevant results by doing so. However, study design must also consider the cost/benefit balance of sequencing whole genomes of a large number of people to high sequence depths, as was done here with the SSC quads (~75X). The previously reported ideal coverage for accurately detecting SNVs is 40-45X where the detection saturates [36]. It has recently been shown that for accurate INDEL detection in personal genomes, whole genome sequencing coverage of 60X may be ideal, at least with 100 bp paired end reads from Illumina [37]. Given the known complexity and heterogeneity of ASD [2,6,9], it is clear that a large study capable of obtaining robust statistical signals is needed; yet a study of this magnitude with 60X coverage is still prohibitively expensive. Our study is useful in terms of contributing a small but rich dataset to larger studies, so that the etiology of ASD can be better understood. While this study was being completed, a study was published using the Complete Genomics (CG) platform to study 85 quartet families with autism [38], although there is a very high false negative rate associated with this sequencing technology, at least with the CG v2.0 pipeline [26].

Methods

Sample collection and sequencing

A pilot study of two SSC families and one Utah family was conducted. The Simons Simplex Collection (SSC) was assembled at 13 clinical centers, with the blood drawn from parents and children (affected and unaffected) sent to the Rutgers University Cell and DNA Repository (RUCDR) for DNA preparation. WGS was performed at CSHL on

the two SSC families using the Illumina HiSeq 2000 platform at an average coverage of 75X, using paired-end 100 bp reads.

The Utah family had previously undergone fragile X screening and Chromosomal Microarray (CMA) genotyping for the proband and mother at the University of Utah. K21 blood samples were collected at the Utah Foundation for Biomedical Research, and genomic DNA was extracted and purified. Finally the DNA was quantified using Qubit dsDNA BR Assay Kit (Invitrogen) and 1 microgram was sent to the CSHL sequencing facility where WGS was performed on the Illumina HiSeq 2000 platform at an average coverage of 40X using paired-end 100 bp reads, and a parallel DNA samples was genotyped with an Illumina Omni2.5 array at the CHOP core facility.

Fragile X analysis (FMR1 test)

The pedigree K21 proband was tested for Fragile X syndrome, a common inherited form of intellectual disability and autism spectrum disorder with characteristic phenotypic features, in which the majority of patients exhibit a massive CGG-repeat expansion mutation in *FMR1* that silences the locus [24]. In order to know if the expansion was present, the fragile X region was amplified by PCR using a single chimeric primer set in which one of the primers is fluorescently labeled. The reactions were then separated by capillary electrophoresis on the ABI310xl Genetic Analyzer and analyzed using the GeneMapper software. Fragile X syndrome can sometimes be misdiagnosed as autism in the absence of the CGG repeat expansion. There are two missense and other point mutations in the FMR1 gene that have been reported and described as causative of Fragile X Syndrome [20-25]. Because missense mutations cannot be detected using the CGG-repeat test and because WGS data was available for every proband, loci spanning *FMR1* were carefully analyzed to see if any of the probands had any possible disease contributing mutation (e.g., p.Ile304Asn, p.Gly266Glu, IVS10+14C→T and p.Ser27X). A CGG repeat analysis on the Fragile X region (chrX: 146,993,468-147,032,646, http://omim.org/entry/309550) was also performed for all the probands to confirm that the CGG repeat number was normal compared to the reference genome. This was done by calling variants and generating a gvcf file with the GATK Haplotype Caller software. The gvcf file contains all sites in the FMR1 gene, whether there is a variant present or not. Using the gvcf file, the gene sequences were inferred and each CGG tri-nucleotide was plotted as it appears within the FMR1 gene region, making evident any subtle difference in the amount or positions of the CGG repeats **(Supp. Fig. 2).** This simple method will only work if the CGG repeat size is covered by the read length of the sequencing technology used to sequence the samples, otherwise it would not align to the reference sequence. However if the reads are not long enough and few or no reads are aligned, we may still infer the presence of an expansion if there is an apparent deletion in the 5' UTR of *FMR1*.

Chromosomal microarray analysis (CMA)

The pedigree K21 proband was genotyped using the Affymetrix Cytogenetics Whole-Genome 2.7 Array, which has a total of 2,141,868 markers across the genome, including 1,742,975 unique non-polymorphic markers and 398,891 SNP markers. After finding a CNV with unknown pathogenicity on chromosome X, the mother was also genotyped using the same array to determine if the CNV was inherited.

SNV and INDEL variant calling

Before proceeding to analyze the WGS data, the quality of raw sequencing reads was assessed using FastQC [http://www.bioinformatics.babraham.ac.uk/projects/fastqc/], which summarizes sequence quality metrics that can indicate whether there was a problem with the sequencing experiment. This quality control procedure is important, as the quality of the raw sequencing data needs to be assessed before performing further downstream analyses. As human genomic variation can range from single nucleotide changes to whole chromosome variations, different analyses need to be performed to retrieve most of the true variation present in each person. In this study, several software packages were used in an integrative manner to analyze all the data generated by the different high throughput technologies. Raw sequence read quality analysis was performed for all samples, followed by aligning them to the reference genome. All analysis prior to the use of variant caller software were applied to the data in a lane by lane fashion; this is done in order to take account for experimental variation introduced by optical duplicates known to occur in a lane specific manner [39].

Whole genome sequence aligning and pre-calling processes

Whole Genome Sequence reads from all samples were aligned, lane by lane, to the GRCh37/hg19 human reference sequence using BWA-MEM 0.7.5a-r405 software [40] with default parameters, tagging shorter split hits as secondary for compatibility with Picard tools used downstream of the alignment. Samples from the SSC families were sequenced to a mean coverage of 75X, with 6 different lanes per sample used to achieve this depth. K21 family samples were sequenced to a mean coverage of 40X, obtained by using 3.5 lanes. The resulting alignments were converted to binary format, then sorted and indexed using SAMtools version 0.1.19-44428cd [41]. Duplicated reads were marked and read groups were assigned to each lane using Picard tools v1.84 [http://sourceforge.net/projects/picard/]. The GATK Indel realigner v3.0-0 was used to correct mapping artifacts that due to reads aligning to the edges of INDELs, may look like evidence for SNPs. The GATK Base Quality Score Recalibrator was also used to correct systematic errors of sequencing technologies [39, 42, 43]. Finally all lanes were merged by sample with Picard tools to generate a ready-to-use alignment.

Variant detection for SNV and INDELS

After obtaining ready-to-use alignments, four different variant callers were used to analyze the WGS data for each individual in the three different families. SNVs and INDELs were called using the GATK Haplotype Caller, v2.8-1 and v3.0-0, with default parameters. GATK Haplotype Caller variants were filtered using the GATK variant quality score recalibration (VQSR) tool. The Freebayes variant caller v9.9.2-43-ga97dbf8 [44] was also used to call SNVs and INDELs on all individuals. Freebayes calls with a QUAL score of less than 30 or with less than 10 supporting reads were filtered out. To further support the detection of *de novo* calls, two other packages were used: Scalpel [45] in *de novo* mode for *de novo* INDEL detection and the Multinomial Analyzer (MA) [13], which implements a multinomial model that considers evidence stemming from all members of a quad to decide whether a call is a true de novo or not. Both Scalpel and the Multinomial Analyzer were used with default parameters and filtering thresholds for MA were set to denovo score>60 and Chi2Pval > 0.0001, as was used in the exome study in which both SSC families were previously analyzed [13]. Variants from the same sample coming from GATK and Freebayes were merged into a single vcf file for

downstream analysis. All variants in the final set were visually inspected on the Golden Helix Genome Browser [Golden Helix GenomeBrowse® visualization tool (Version 2.0.4)]

Variant classification and prioritization

The final set of high quality calls were divided into different models of inheritance, so that the way in which the mutations emerged and how they were possibly contributing to the condition could be interrogated. After obtaining model-specific subsets, the variants were annotated with a Combined Annotation Dependent Depletion (CADD) score, a metric that evaluates the deleteriousness of SNVs as well as INDELs variants in the human genome. CADD scores are generated by integrating multiple annotations, including PolyPhen and SIFT scores, into one metric by contrasting variants that survived natural selection with simulated mutations [46]. Those variants with a CADD score of greater than 20 were kept as potentially deleterious, and the number of reads supporting each variant was compared among all family members to decide whether a call was a false positive or not. All variants were further filtered using a MAF < 0.01 from the 1000 genomes project (Oct 2014). The final set of variants was annotated with in-house tools as well as the ANNOVAR software [47] using the UCSC [48] and RefSeq [49] gene tables, the SSC [50], Exome Variant Server [http://evs.gs.washington.edu/EVS/] and ClinVar databases [51] and the recently released ExAC database [http://exac.broadinstitute.org)].

Models

There are several ways in which a disease-contributing genetic variant can be present in an individual. As we were not only interested in the variants, but also in their origin, they were divided into different models before prioritization.

De Novo Model

De novo variants are those that emerge at some stage during the gametogenesis of one of the parents or embryogenesis of the child, so those mutations will be only present in the offspring and not the parents. Only those variants present uniquely in the proband and not in parents or unaffected sibling were kept for downstream annotation and analysis.

X-Linked

Here only variants on chromosome X are considered. As all of the probands in this study are males, the only X chromosome copy they have comes from the mother, who by having two X chromosome copies could be masking the deleteriousness of a mutation, which is then expressed fully in the male offspring. All X chromosome variants present in the proband inherited from the mother but not present in the healthy sibling or father were kept for downstream annotation and analysis.

Autosomal Recessive

In this model, a given variant is required to be present in both probands with one copy inherited by the mother and the second one from the father. The autosomal recessive variants found in the healthy sibling are also excluded.

Compound Heterozygous

Sometimes a gene can bear two different heterozygous mutations; one in each chromosomal copy, affecting both copies of a gene but not with the same exact mutation, as is the case for the autosomal recessive model. For this set of variants, only those combinations of heterozygous mutations on the same gene and present in the proband were considered.

Mitochondrial

In a similar fashion as chromosome X, it is well known that the mitochondrial DNA is passed from mother to offspring; however in this case, if a mutation is contributing to the disease the mother would also be affected so the only mitochondrial mutations considered are under the de novo model described above.

VEP-GEMINI

The VEP (Variant Effect Predictor)-Genome Mining (GEMINI) [52] toolset is a framework for annotating and prioritizing genomic variants by different criteria. Built-in analysis tools were used to obtain variants characterized by different classifications: *de novo*, compound heterozygous, autosomal recessive and impact severity. The VEP-GEMINI toolset was used to get additional information about each variant, and to compare the results obtained with the model classifications and prioritizations performed with in-house tools. The criteria for keeping variants from each classification scheme were for variants to have a CADD score of greater than 20 or be annotated as having high impact severity for the proband.

Variant calling for copy number variants

The Estimation by Read Depth with SNVs (ERDS) software [53] was used with default parameters to call CNVs from WGS data on each individual. It uses WGS data along with previously generated vcf files using the read depth and number of contiguous heterozygous and homozygous SNVs to call CNVs. Only calls with an ERDS score of > 300 were kept.

Additionally, CNVs were called with the microarray data from pedigree K21, which was genotyped with an Illumina Omni2.5 array and analyzed with the software package PennCNV [54]. For kilobase-resolution detection of CNVs, PennCNV uses an algorithm that implements a hidden Markov model, which integrates multiple signal patterns across the genome and uses the distance between neighboring SNPs and the allele frequency of SNPs. The two signal patterns that it uses are the Log R Ratio (LRR), which is a normalized measure of the total signal intensity for two alleles of the SNP and the B Allele Frequency (BAF), a normalized measure of the allelic intensity ratio of two alleles. The combination of both signal patterns is then used to infer copy number changes in the genome. Microarrays often show variation in hybridization intensity (genomic waves), which is related to the genomic position of the clones, and that correlates to GC content among the genomic features considered. For adjustment of such genomic waves in signal intensities, the cal_gc_snp.pl PennCNV program was used to generate a GC model that considered the GC content surrounding each Illumina Omni2.5 marker within 500kb on each side (1Mb total). The joint-calling algorithm designed for parents-offspring trios was used, as it is the most accurate of the algorithms in the package for family based studies. The Hidden Markov Model used is contained in the hhall.hmm file provided by the latest PennCNV package, and the custom Population Frequency of B

allele (PFB) file for all the SNPs in the Illumina Omni2.5 array was generated from 600 controls (which consists of 600 unaffected parents from the Simons Simplex Collection (provided by Dr. Stephan Sanders from Yale University). The GC model described above was also used during CNV calling.

Chromosome X CNVs were called separately using the -- test mode with the --chrx option. Using BEDtools [55] and in-house tools, consensus CNV calls were obtained for parents from the two separate trio calling processes that had to be done for each child in the quad. CNVs were quality filtered by considering the length of the CNV event (for both algorithms: ERDS and PennCNV) and for microarray data, the number of SNPs embedded on the CNV region and the number of expected SNPs for that given region **(Supp. Fig. 5)**, histocompatibility regions, centromeric and telomeric regions were also filtered out as it is common to find non-pathogenic variants there (both algorithms).

For Pedigree K21, ERDS and PennCNV calls were compared and the union of each pipeline's set of variants was annotated with in-house tools and the ANNOVAR software [47] using dbVar [56] , DGV [57], ClinVar [51], DECIPHER [58], ENCODE [35] and the SFARIgene databases [50] and those variants which $\geq$ 90% of their total length overlapped reciprocally with variants found in controls were ruled out. ERDS filtered output for pedigrees SSC_1 and SSC_2 were annotated with the same software and criteria.

Sanger Sequencing

PCR primers for the Chr17:4458481(hg19) variant in *MYBBP1A* were designed to produce a 911 bp amplicon, using Primer 3 (http://primer3.sourceforge.net). Primers were obtained from Sigma-Aldrich®, and tested for PCR efficiency with an in-house DNA sample using a Phusion Flash High-Fidelity PCR Master Mix (Life Technologies, USA). The optimized PCR reaction was then carried out on patient DNA. PCR products were visually inspected for amplification efficiency using agarose gel electrophoresis, and were purified using the QIAquick PCR Purification Kit (QIAGEN Inc., USA). Purified products were then diluted to 5~10 ng/µl in water for use with the ABI 3700 sequencer. The resulting *.ab1 sequence files were loaded into the CodonCode Aligner V5.1.2 for analysis. All sequence traces were manually reviewed to ensure the reliability of the genotype calls.

List of abbreviations used

Single-nucleotide polymorphism (SNP), copy number variation (CNV), insertions and deletions (INDELs), structual variant (SV), whole genome sequencing (WGS), whole exome sequencing (WES), next-generation sequencing (NGS), bp (base pair), Kb (kilo base pairs), Mb (megabase pair), PCR (polymerase chain reaction)

Additional Information

Data Deposition and Access

All of the sequence reads can be downloaded under project accession number

[PRJNA282537] from the Sequence Read Archive (http://www.ncbi.nlm.nih.gov/sra).

SRA Bioproject: PRJNA282537
Biosamples: SAMN03571202, SAMN03571214, SAMN03571217, SAMN03571219

Online Resources:

1000G database: http://www.1000genomes.org/

Exome Aggregation Consortium (ExAC): http://exac.broadinstitute.org/

Ethics compliance

Research was carried out in compliance with the Helsinki Declaration. Two of the families analyzed in this study belong to the SSC (referred as SSC_1 & SSC_2), and both families were clinically evaluated and extensively phenotyped as well as whole exome sequenced for a previous study [13].

The third family (referred to as K_21) was recruited to this study at the Utah Foundation for Biomedical Research (UFBR) where extensive clinical evaluation was performed. Written consent was obtained for phenotyping and whole genome sequencing through Protocol #100 at the Utah Foundation for Biomedical Research, approved by the Independent Investigational Review Board, Inc.

Acknowledgments

Dr. Stephan Sanders provided the PFB file necessary for CNV calling. Dr. Kai Wang assisted in the CNV analysis. The authors would like to thank the Exome Aggregation Consortium and the groups that provided exome variant data for comparison. A full list of contributing groups can be found at http://exac.broadinstitute.org/about.

Author Contributions

Jiménez-Barrón L.T. developed the study design, performed all informatics analyses and wrote the manuscript. O'Rawe J. provided in-house tools, contributed to the study design and revised the manuscript. Yiyang Wu performed the sanger sequencing validation experiment. H. Fang participated in the study design. Iossifov I. provided the SSC data. G.J.L. participated in the study design, data interpretation, and manuscript writing.

Funding

The laboratory of G.J.L. is supported by funds from the Stanley Institute for Cognitive Genomics at Cold Spring Harbor Laboratory (CSHL). The CSHL genome center is supported in part by a Cancer Center Support Grant (CA045508) from the NCI.

Competing Interests

G.J.L serves on advisory boards for GenePeeks, Inc. and Omicia, Inc.

References

1. Baio, J., *Prevalence of autism spectrum disorder among children aged 8 years - autism and developmental disabilities monitoring network, 11 sites, United States, 2010.* MMWR Surveill Summ, 2014. **63**(2): p. 1-21.
2. Zhao, X., et al., *A unified genetic theory for sporadic and inherited autism.* Proc Natl Acad Sci U S A, 2007. **104**(31): p. 12831-6.
3. Gilman, S.R., et al., *Rare de novo variants associated with autism implicate a large functional network of genes involved in formation and function of synapses.* Neuron, 2011. **70**(5): p. 898-907.
4. Levy, D., et al., *Rare de novo and transmitted copy-number variation in autistic spectrum disorders.* Neuron, 2011. **70**(5): p. 886-97.
5. Zaroff, C.M. and S.Y. Uhm, *Prevalence of autism spectrum disorders and influence of country of measurement and ethnicity.* Soc Psychiatry Psychiatr Epidemiol, 2012. **47**(3): p. 395-8.
6. Bernier, R., et al., *Disruptive CHD8 mutations define a subtype of autism early in development.* Cell, 2014. **158**(2): p. 263-76.
7. Zhou, J. and L.F. Parada, *PTEN signaling in autism spectrum disorders.* Curr Opin Neurobiol, 2012. **22**(5): p. 873-9.
8. Betancur, C., *Etiological heterogeneity in autism spectrum disorders: more than 100 genetic and genomic disorders and still counting.* Brain Res, 2011. **1380**: p. 42-77.
9. O'Roak, B.J., et al., *Multiplex targeted sequencing identifies recurrently mutated genes in autism spectrum disorders.* Science, 2012. **338**(6114): p. 1619-22.
10. Lyon, G.J. and J. O'Rawe, *Human genetics and clinical aspects of neurodevelopmental disorders*, in *The Genetics of Neurodevelopmental Disorders*, K. Mitchell, Editor. 2015, Wiley Press.
11. Robinson, E.B., et al., *Autism spectrum disorder severity reflects the average contribution of de novo and familial influences.* Proc Natl Acad Sci U S A, 2014. **111**(42): p. 15161-5.
12. Neale, B.M., et al., *Patterns and rates of exonic de novo mutations in autism spectrum disorders.* Nature, 2012. **485**(7397): p. 242-5.
13. Iossifov, I., et al., *De novo gene disruptions in children on the autistic spectrum.* Neuron, 2012. **74**(2): p. 285-99.
14. Sugathan, A., et al., *CHD8 regulates neurodevelopmental pathways associated with autism spectrum disorder in neural progenitors.* Proc Natl Acad Sci U S A, 2014. **111**(42): p. E4468-77.
15. Rothwell, P.E., et al., *Autism-associated neuroligin-3 mutations commonly impair striatal circuits to boost repetitive behaviors.* Cell, 2014. **158**(1): p. 198-212.
16. Iossifov, I., et al., *The contribution of de novo coding mutations to autism spectrum disorder.* Nature, 2014. **515**(7526): p. 216-21.
17. Ronemus, M., et al., *The role of de novo mutations in the genetics of autism spectrum disorders.* Nat Rev Genet, 2014. **15**(2): p. 133-41.
18. Fischbach, G.D. and C. Lord, *The Simons Simplex Collection: a resource for identification of autism genetic risk factors.* Neuron, 2010. **68**(2): p. 192-5.
19. Sherry, S.T., et al., *dbSNP: the NCBI database of genetic variation.* Nucleic Acids Res, 2001. **29**(1): p. 308-11.
20. Collins, S.C., et al., *Identification of novel FMR1 variants by massively parallel sequencing in developmentally delayed males.* Am J Med Genet A, 2010. **152A**(10): p. 2512-20.
21. De Boulle, K., et al., *A point mutation in the FMR-1 gene associated with fragile X mental retardation.* Nat Genet, 1993. **3**(1): p. 31-5.

22. Gronskov, K., et al., *A nonsense mutation in FMR1 causing fragile X syndrome.* Eur J Hum Genet, 2011. **19**(4): p. 489-91.
23. Lugenbeel, K.A., et al., *Intragenic loss of function mutations demonstrate the primary role of FMR1 in fragile X syndrome.* Nat Genet, 1995. **10**(4): p. 483-5.
24. Myrick, L.K., et al., *Fragile X syndrome due to a missense mutation.* Eur J Hum Genet, 2014. **22**(10): p. 1185-9.
25. Wang, Y.C., et al., *Novel point mutation within intron 10 of FMR-1 gene causing fragile X syndrome.* Hum Mutat, 1997. **10**(5): p. 393-9.
26. O'Rawe, J., et al., *Low concordance of multiple variant-calling pipelines: practical implications for exome and genome sequencing.* Genome Med, 2013. **5**(3): p. 28.
27. Assmus, J., et al., *Equivalent indels--ambiguous functional classes and redundancy in databases.* PLoS One, 2013. **8**(5): p. e62803.
28. Tan, A., G.R. Abecasis, and H.M. Kang, *Unified representation of genetic variants.* Bioinformatics, 2015.
29. Hu, H., et al., *VAAST 2.0: improved variant classification and disease-gene identification using a conservation-controlled amino acid substitution matrix.* Genet Epidemiol, 2013. **37**(6): p. 622-34.
30. Favier, D. and T.J. Gonda, *Detection of proteins that bind to the leucine zipper motif of c-Myb.* Oncogene, 1994. **9**(1): p. 305-11.
31. Maglott, D., et al., *Entrez Gene: gene-centered information at NCBI.* Nucleic Acids Res, 2005. **33**(Database issue): p. D54-8.
32. Magrane, M. and U. Consortium, *UniProt Knowledgebase: a hub of integrated protein data.* Database (Oxford), 2011. **2011**: p. bar009.
33. Mori, S., et al., *Myb-binding protein 1A (MYBBP1A) is essential for early embryonic development, controls cell cycle and mitosis, and acts as a tumor suppressor.* PLoS One, 2012. **7**(10): p. e39723.
34. Kim, J.W., et al., *LAMB3 mutations causing autosomal-dominant amelogenesis imperfecta.* J Dent Res, 2013. **92**(10): p. 899-904.
35. Rosenbloom, K.R., et al., *ENCODE data in the UCSC Genome Browser: year 5 update.* Nucleic Acids Res, 2013. **41**(Database issue): p. D56-63.
36. Ajay, S.S., et al., *Accurate and comprehensive sequencing of personal genomes.* Genome Res, 2011. **21**(9): p. 1498-505.
37. Fang, H., et al., *Reducing INDEL calling errors in whole genome and exome sequencing data.* Genome Med, 2014. **6**(10): p. 89.
38. Yuen, R.K., et al., *Whole-genome sequencing of quartet families with autism spectrum disorder.* Nat Med, 2015. **21**(2): p. 185-91.
39. McKenna, A., et al., *The Genome Analysis Toolkit: a MapReduce framework for analyzing next-generation DNA sequencing data.* Genome Res, 2010. **20**(9): p. 1297-303.
40. Li, H. and R. Durbin, *Fast and accurate short read alignment with Burrows-Wheeler transform.* Bioinformatics, 2009. **25**(14): p. 1754-60.
41. Li, H., et al., *The Sequence Alignment/Map format and SAMtools.* Bioinformatics, 2009. **25**(16): p. 2078-9.
42. DePristo, M.A., et al., *A framework for variation discovery and genotyping using next-generation DNA sequencing data.* Nat Genet, 2011. **43**(5): p. 491-8.
43. Van der Auwera, G.A., et al., *From FastQ data to high confidence variant calls: the Genome Analysis Toolkit best practices pipeline.* Curr Protoc Bioinformatics, 2013. **11**(1110): p. 11 10 1-11 10 33.
44. Garrison, E. and G. Marth, *Haplotype-based variant detection from short-read sequencing.* arXiv preprint arXiv:1207.3907, 2012.
45. Narzisi, G., et al., *Accurate de novo and transmitted indel detection in exome-capture data using microassembly.* Nat Methods, 2014. **11**(10): p. 1033-6.

46. Kircher, M., et al., *A general framework for estimating the relative pathogenicity of human genetic variants.* Nat Genet, 2014. **46**(3): p. 310-5.
47. Wang, K., M. Li, and H. Hakonarson, *ANNOVAR: functional annotation of genetic variants from high-throughput sequencing data.* Nucleic Acids Res, 2010. **38**(16): p. e164.
48. Kent, W.J., et al., *The human genome browser at UCSC.* Genome Res, 2002. **12**(6): p. 996-1006.
49. Raney, B.J., et al., *Track data hubs enable visualization of user-defined genome-wide annotations on the UCSC Genome Browser.* Bioinformatics, 2014. **30**(7): p. 1003-5.
50. Basu, S.N., R. Kollu, and S. Banerjee-Basu, *AutDB: a gene reference resource for autism research.* Nucleic Acids Res, 2009. **37**(Database issue): p. D832-6.
51. Landrum, M.J., et al., *ClinVar: public archive of relationships among sequence variation and human phenotype.* Nucleic Acids Res, 2014. **42**(Database issue): p. D980-5.
52. Paila, U., et al., *GEMINI: integrative exploration of genetic variation and genome annotations.* PLoS Comput Biol, 2013. **9**(7): p. e1003153.
53. Zhu, M., et al., *Using ERDS to infer copy-number variants in high-coverage genomes.* Am J Hum Genet, 2012. **91**(3): p. 408-21.
54. Wang, K., et al., *PennCNV: an integrated hidden Markov model designed for high-resolution copy number variation detection in whole-genome SNP genotyping data.* Genome Res, 2007. **17**(11): p. 1665-74.
55. Quinlan, A.R. and I.M. Hall, *BEDTools: a flexible suite of utilities for comparing genomic features.* Bioinformatics, 2010. **26**(6): p. 841-2.
56. Lappalainen, I., et al., *DbVar and DGVa: public archives for genomic structural variation.* Nucleic Acids Res, 2013. **41**(Database issue): p. D936-41.
57. MacDonald, J.R., et al., *The Database of Genomic Variants: a curated collection of structural variation in the human genome.* Nucleic Acids Res, 2014. **42**(Database issue): p. D986-92.
58. Firth, H.V., et al., *DECIPHER: Database of Chromosomal Imbalance and Phenotype in Humans Using Ensembl Resources.* Am J Hum Genet, 2009. **84**(4): p. 524-33.

Table 1. **Body measurements and IQ tests scores.**

Proband	BMI	Head Circumference	Height	Weight	Race	Proband IQ	Proband VIQ	Proband NVIQ
SSC_2	17.4	51.6	102	18.1	Asian	61	32	89
SSC_1	32.9	60.5	175	100.9	Caucasian	120	136	108
K_21	NA	NA	NA	NA	Caucasian	NA	NA	NA

Table 2. **The Aberrant Behavior Checklist scores for each Proband.**

Proband	ABC I: Irritability	ABC II: Lethargy	ABC III: Stereotypy	ABC IV: Hyperactivity	ABC V: Inappropriate Speech
SSC_2	8	13	5	27	0
SSC_1	14	5	3	6	6
K_21	NA	NA	NA	NA	NA

Table 3. **The Autism Diagnostic Observation Schedule (ADOS) scores for each Simon's Simplex Collection Proband.**

Proband	ADOS1 Algorithm	ADOS Communication	ADOS Reciprocal Social
SSC_2	no-words	7	11
SSC_1	NA	3	8
K_21	NA	NA	NA

Table 4. **The Child Behavior Checklist scores for each Simon's Simplex Collection Proband.**

Proband	ADD/ ADHD	Aggressive Behavior	Anxiety Problems	Anxious/ Depressed	Attention Problems	Defiant	Withdrawn	Total Problems
SSC_2	52	55	51	56	53	59	82	61
SSC_1	57	70	58	63	51	66	63	66
K_21	NA	NA	NA	NA	NA	NA	NA	NA

Table 5. The Vineland Adaptive Behavior Scale scores for each Simon's Simplex Collection Proband.

Proband	Communication	Daily Living Skills	Motor Skills	Socialization
SSC_2	76	58	100	63
SSC_1	81	89	NA	73
K_21	NA	NA	NA	NA

Table 6. Number of variants obtained by each algorithm before and after filtering.

Variants	GATK HC	Freebayes	Intersection	Unique to GATK %	Unique to Freebayes %	Intersection %
Raw SNVs	3,911,804	4,216,193	3,593,919	13.7	7	79.3
Filtered SNVs	3,403,728	3,714,842	3,255,217	11.9	3.8	84.3
Raw Indels	814,730	790,178	580,335	20.5	22.9	56.6
Filtered Indels	725,573	720,426	542,982	19.7	20.2	60.1

Table 7. De Novo Indels.

Algorithm	De Novo Indels
HC u FB	52933
Scalpel	26
Intersection	4

Table 8. **Final set of SNV.**

Model	Ref -> Alt/ Effect	Location hg19	Affected Gene	Algorithms that called the variant	Pedigree ID	ExAC Allele Frequency	CADD score
De Novo	Sub(C->T) missense	Chr1:209823359	LAMB3	Freebayes Multinomial Analyzer GATK	SSC_2 (**12605**)	0	22.7
De Novo	Sub(G->A) nonsense	Chr17:4458481	MYBBP1A	Freebayes Multinomial Analyzer GATK	K21	1/74014=0.00001351	40

Table 9. **Previous SSC Exome Study Comparison.**

Family ID	Location	Ref -> Alt/ Effect	Genes	Population type	GATK_HC/ Filtered	Freebayes/ Filtered	MA/ Filtered	CAAD Score
12605	10:103908608	sub (C->T)/ missense	PPRC1	denovo	yes/NO	yes/yes	yes/yes	19.5
12605	1:209823359	sub (A->C)/ missense	LAMB3	denovo	yes/yes	yes/yes	yes/yes	22.7
12605	3:185993461	sub (G->T)/ intron	DGKG	denovo	yes/NO	yes/yes	yes/yes	7.5

Figure Legends

Figure 1. (a) Pedigree structure of a Simplex Autism Family. For a family to be classified as a Simplex Autism Family, it has to be composed of one affected child and at least one unaffected sibling, and both parents do not have obvious autism. Probands and siblings can be either males or females. **(b) K_21 Proband showing no dysmorphology. (c) Analyzed Pedigrees.** Two of the families have male probands and unaffected male siblings (K_21 and SSC_1), whereas the third family has a male proband and a female unaffected sibling (SSC_2).

Figure 2. **A conceptual map of human sequence variation**. Here, we show approximate sizes, as well as the associated signature, of the various different types of human sequence variation that can be currently detected with the WGS, microarray sequencing and informatics technologies employed in this work. The frequency axis shows the approximate frequency of the various genetic variation types that are currently detectable via germline WGS combined with microarray sequencing. Above the visual signatures of the different types of human sequence variation, the general names of the different informatics software tools for detecting the variation are noted which include, the Genome Analysis Took Kit (GATK), Scalpel, PennCNV, the estimation by read depth with single-nucleotide variants (ERDS) CNV caller and the FreeBayes caller.

Figure 3. Genome Browser Screen cut for the read depths in the **MYBBP1A stop gain. (**chr17:4458481) mutation in K21 family.

Figure 4. (a). Genome Browser Screen cut for the read depths in the LAMB3 missense mutation (chr1:209823359). **(b).** Genome Browser screen cut showing 34 reads supporting the variant for the proband in SSC_1 family.

Figure 5. (a). Genome Browser Screen cut for the Read Depths in the K21 CNV 3q22.1 region of 16Kb. **(b).** B Allele Frequencies values for Illumina Omni 2.5 markers on 3q22.1 region including the markers belonging to the CNV region detected by ERDS in red. **(c).** Log R Ratio values for Illumina Omni 2.5 markers on 3q22.1 region including the markers belonging to the CNV region detected by ERDS in red.

Figure 6. (a) Genome Browser Screen cut for the Read Depths in the K21 CNV 16p12.3 region of 22Kb. (**b)** B Allele Frequencies values for Illumina Omni 2.5 markers on K21 16p12.3 region including the markers belonging to the CNV region detected by ERDS in red. **(c).** Log R Ratio values for Illumina Omni 2.5 markers on K21 16p12.3 region including the markers belonging to the CNV region detected by ERDS in red.

Figure 7. Genome Browser Screen cut for the Read Depths in the SSC_2 CNV 4p16.3 region of 50Kb. The highlighted region is where the 4 people bear either a homozygous or heterozygous deletion, only the Proband has an homozygous deletion of the complete deletion region, which could have been generated by inheriting the deleted copy from both parents.

Figures

Figure 1.

(a)

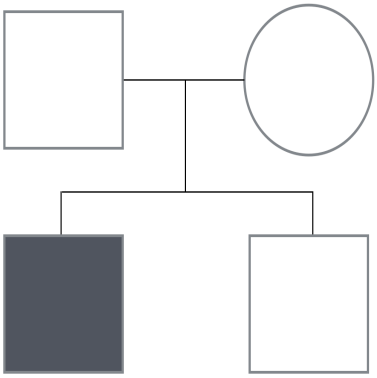

(b) removed for medicolegal reasons

Will appear in final paper.

(c)

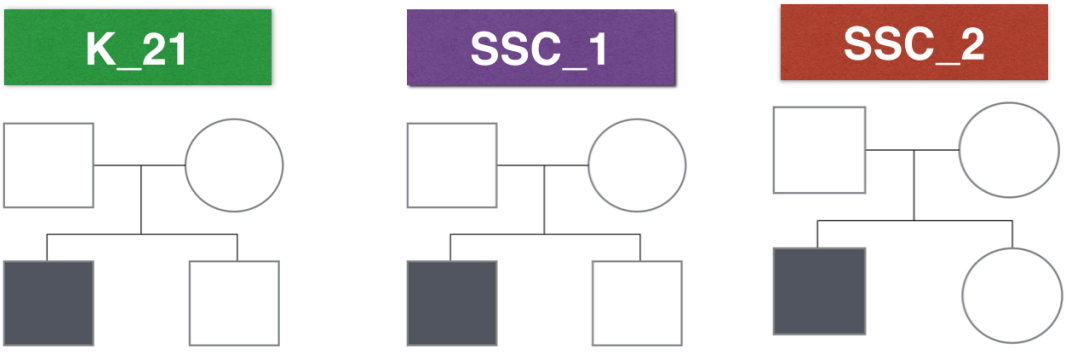

Figure 2

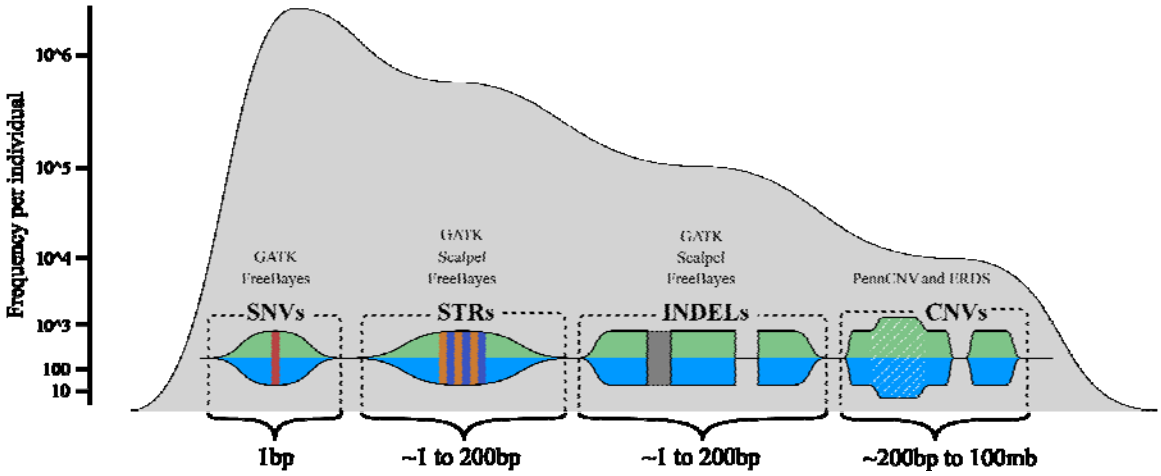

Figure 3.

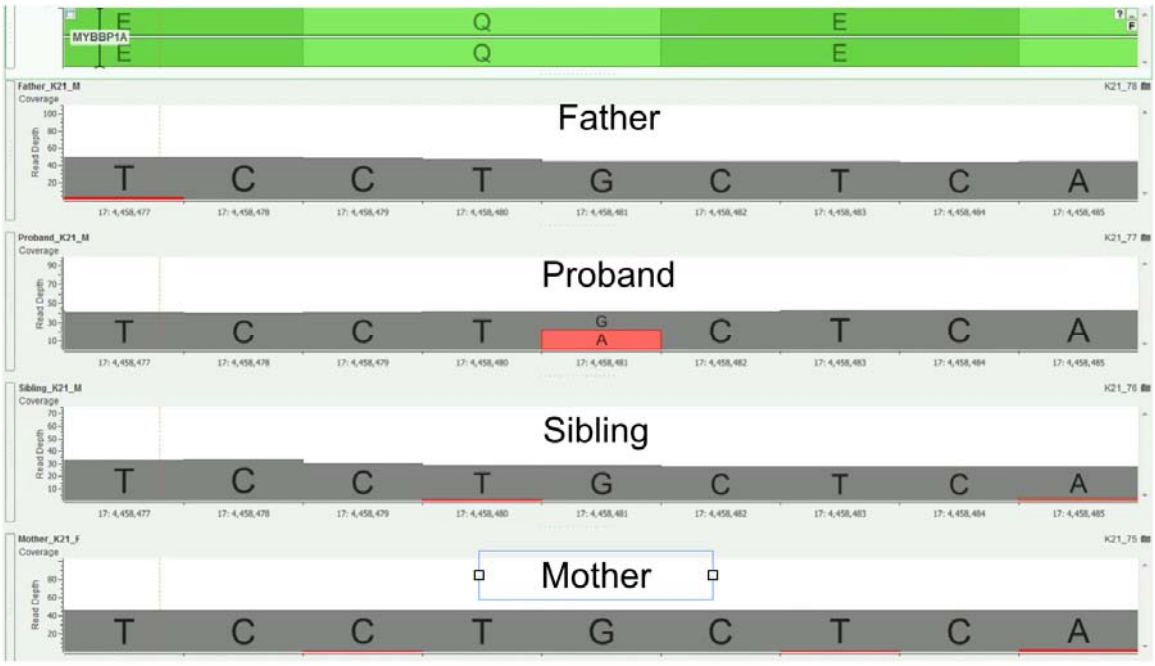

Figure 4.

(a)

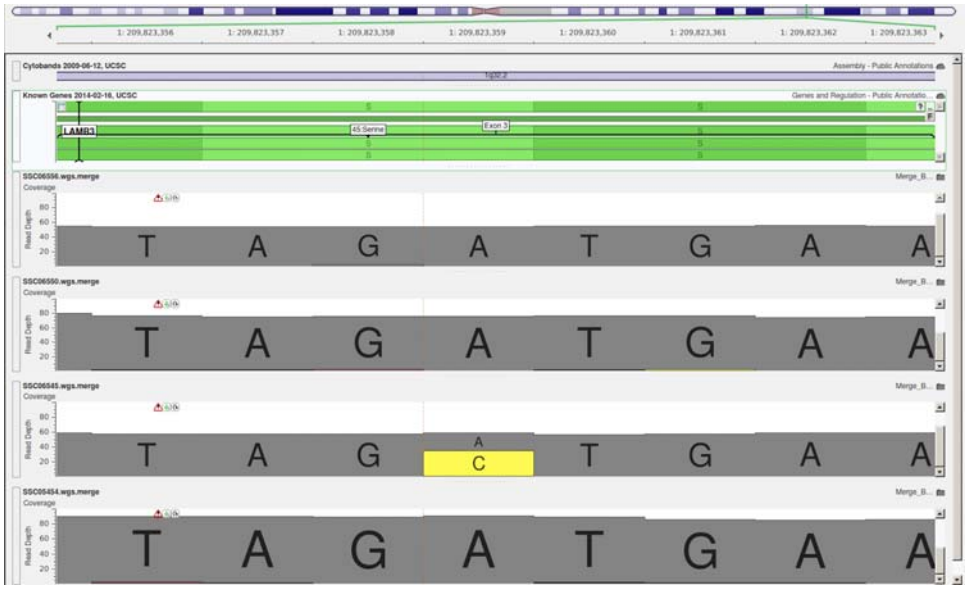

(b)

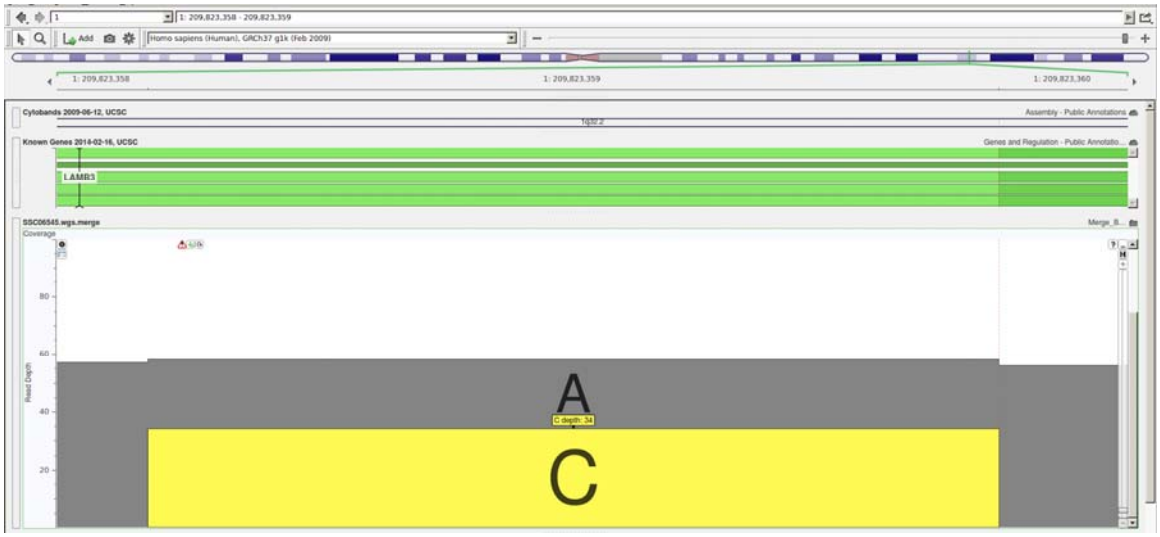

Figure 5.

(a)

(b)

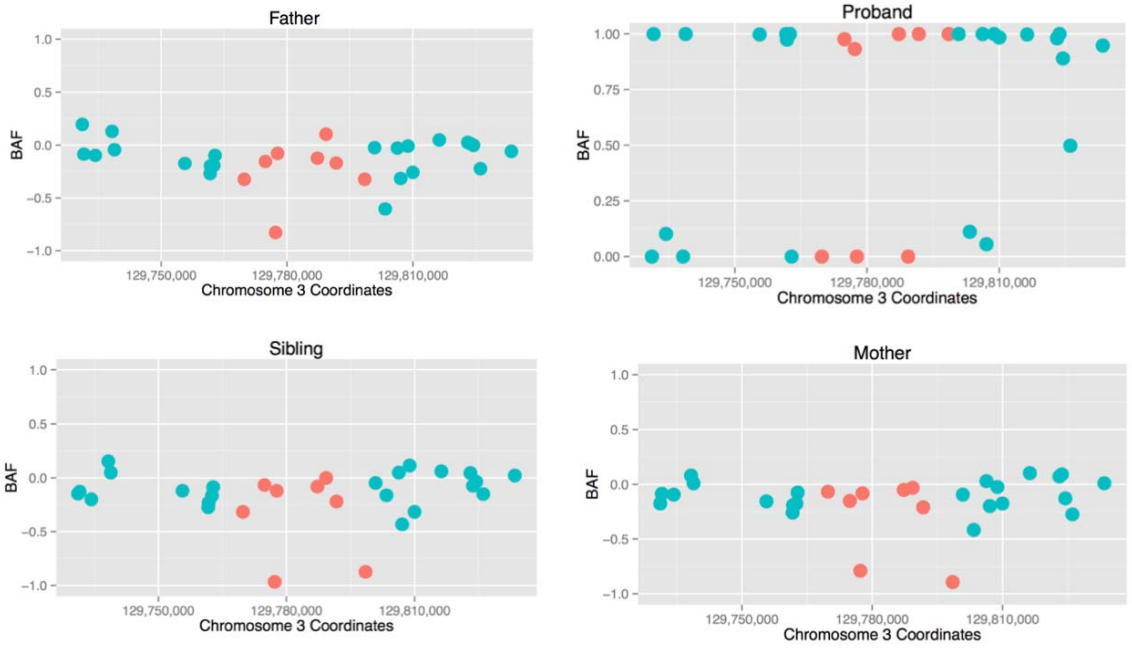

(c)

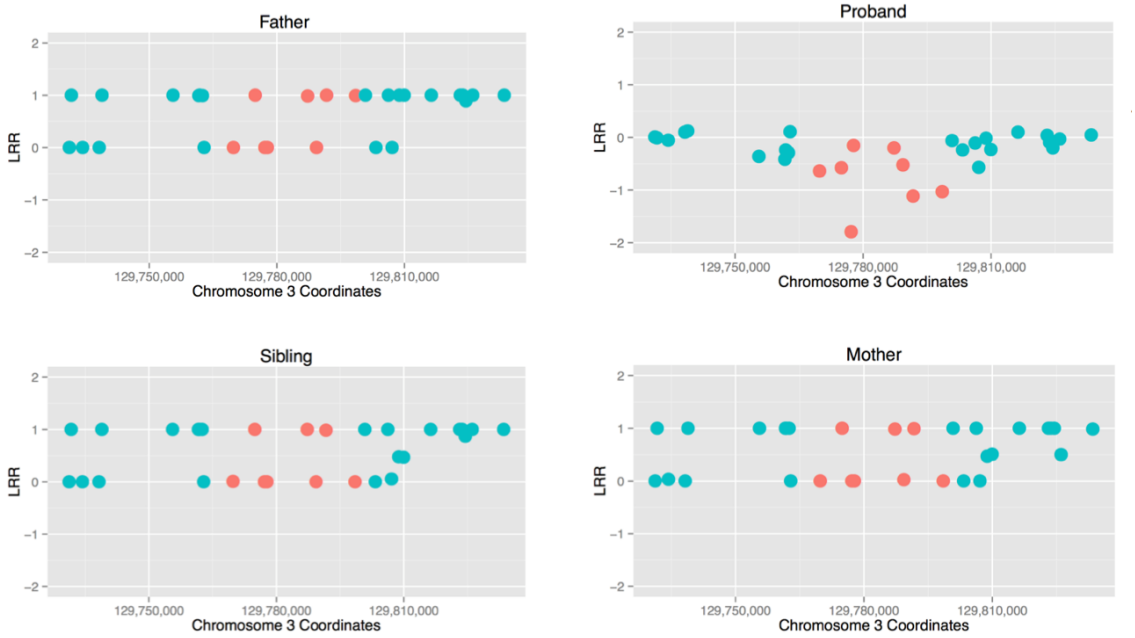

Figure 6.

(a)

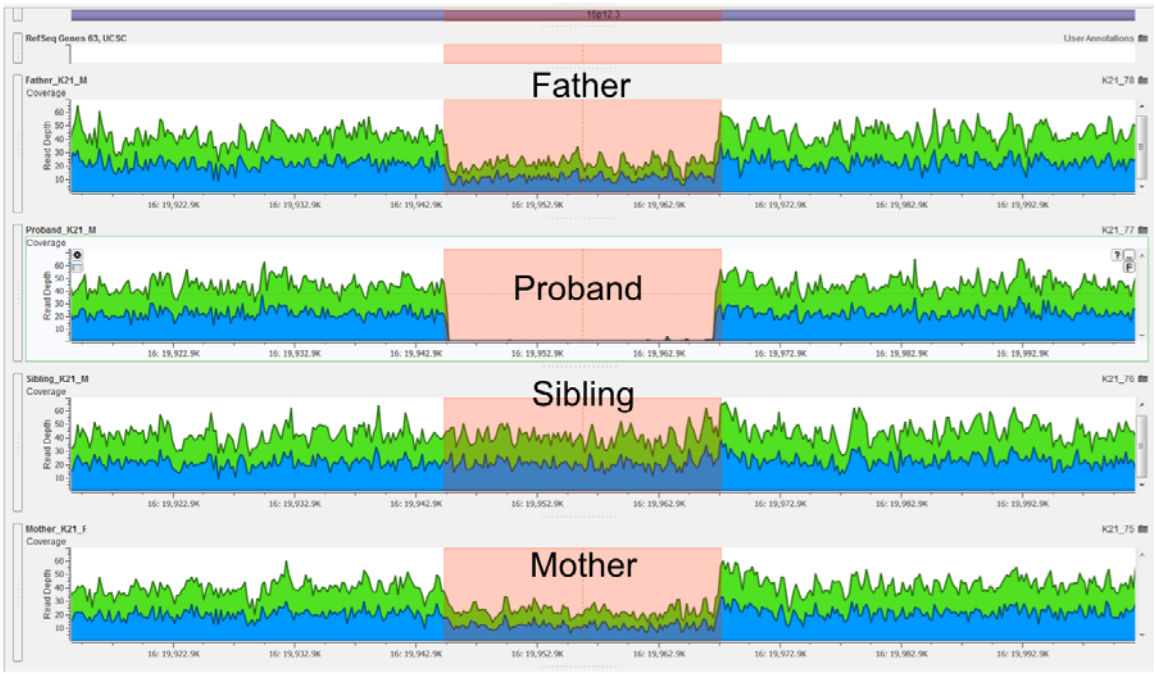

(b)

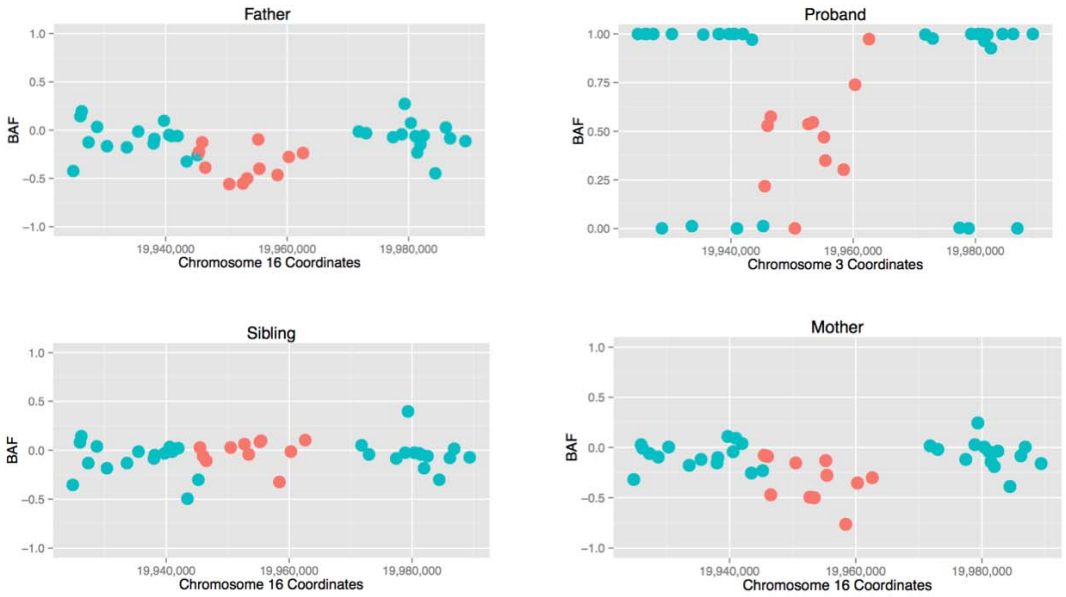

(c)

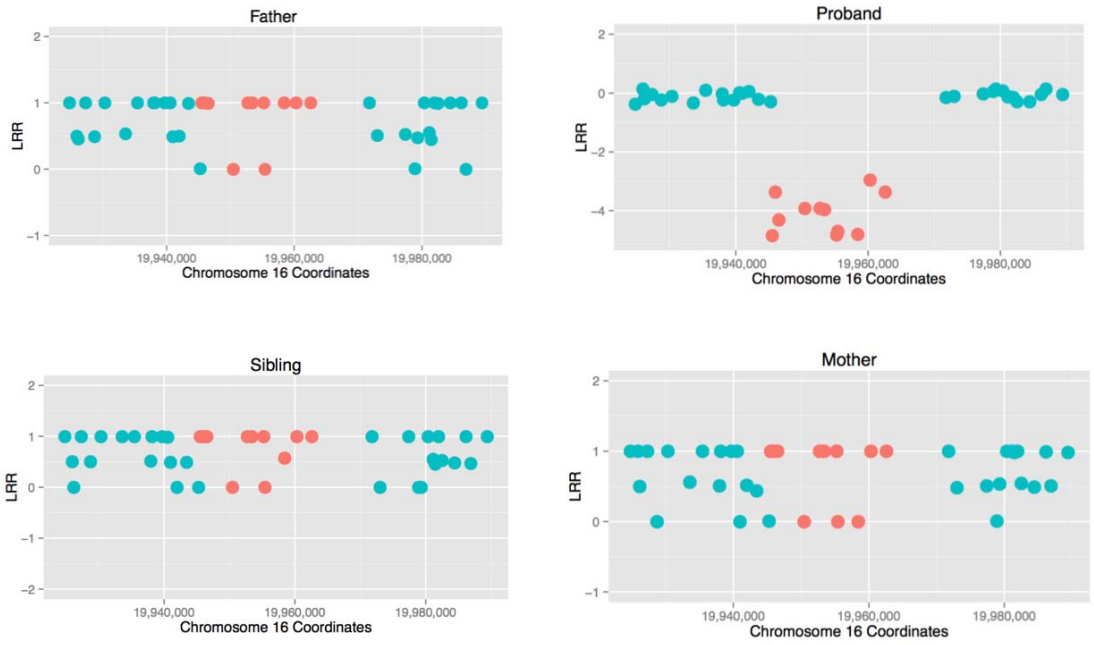

Figure 7.

Supplemental Figures

Supplemental Figure 1.

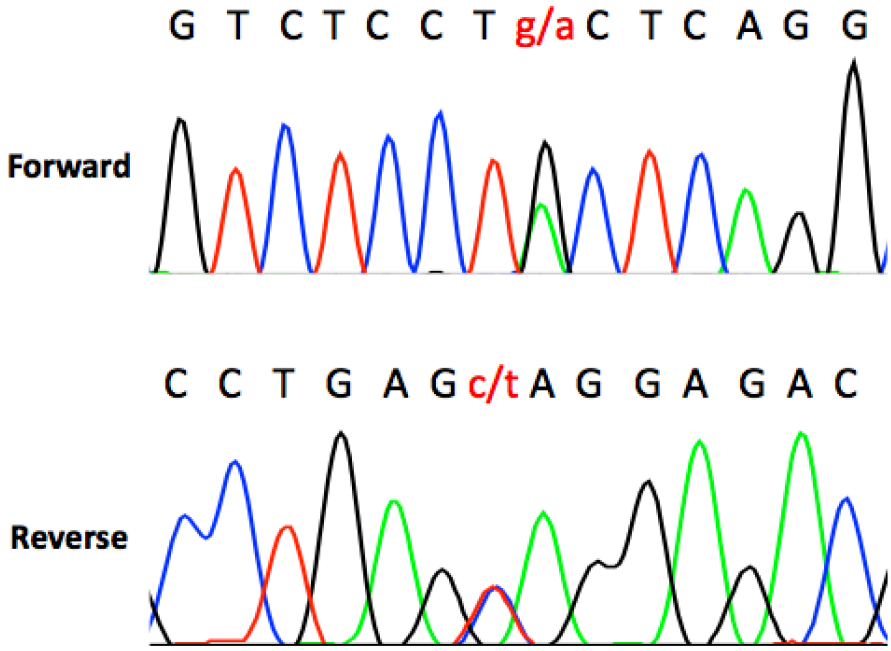

Supplemental Figure 2.

(a)

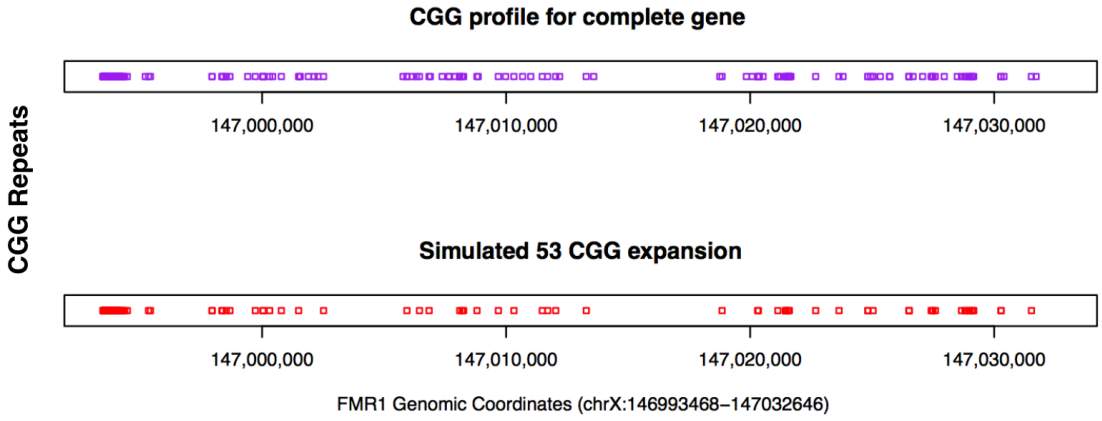

(b)

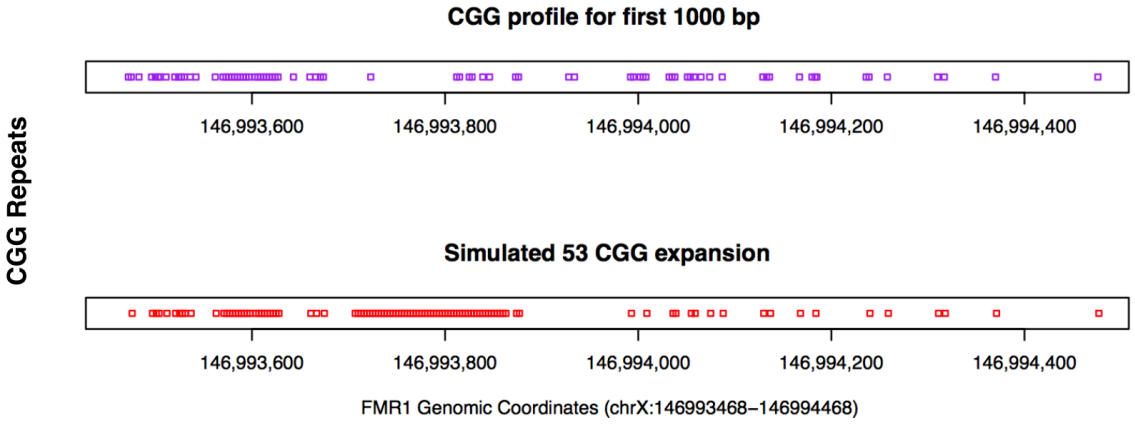

Supplemental Figure 3.

Supplemental Figure 4.

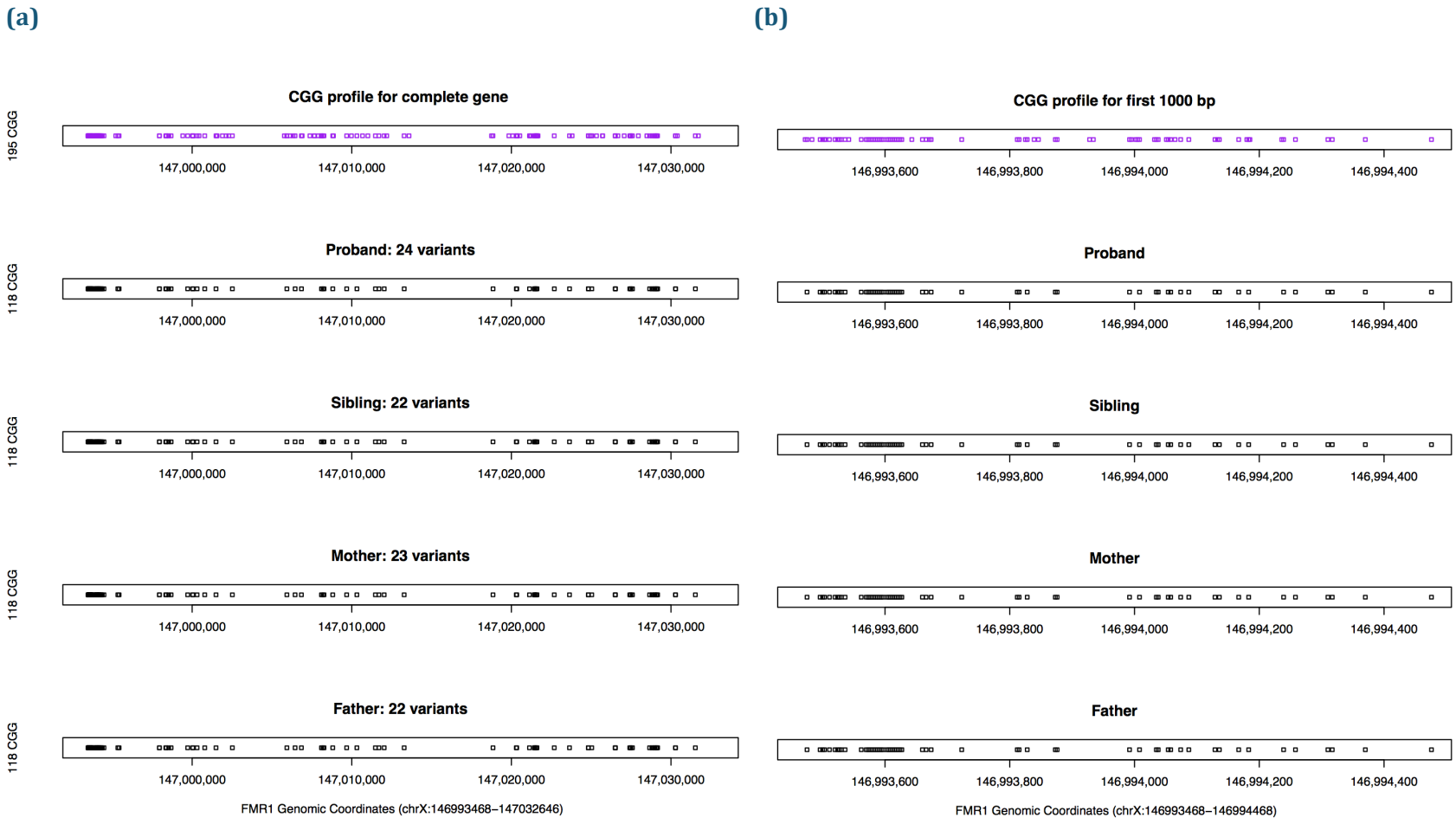

Supplemental Figure 5.

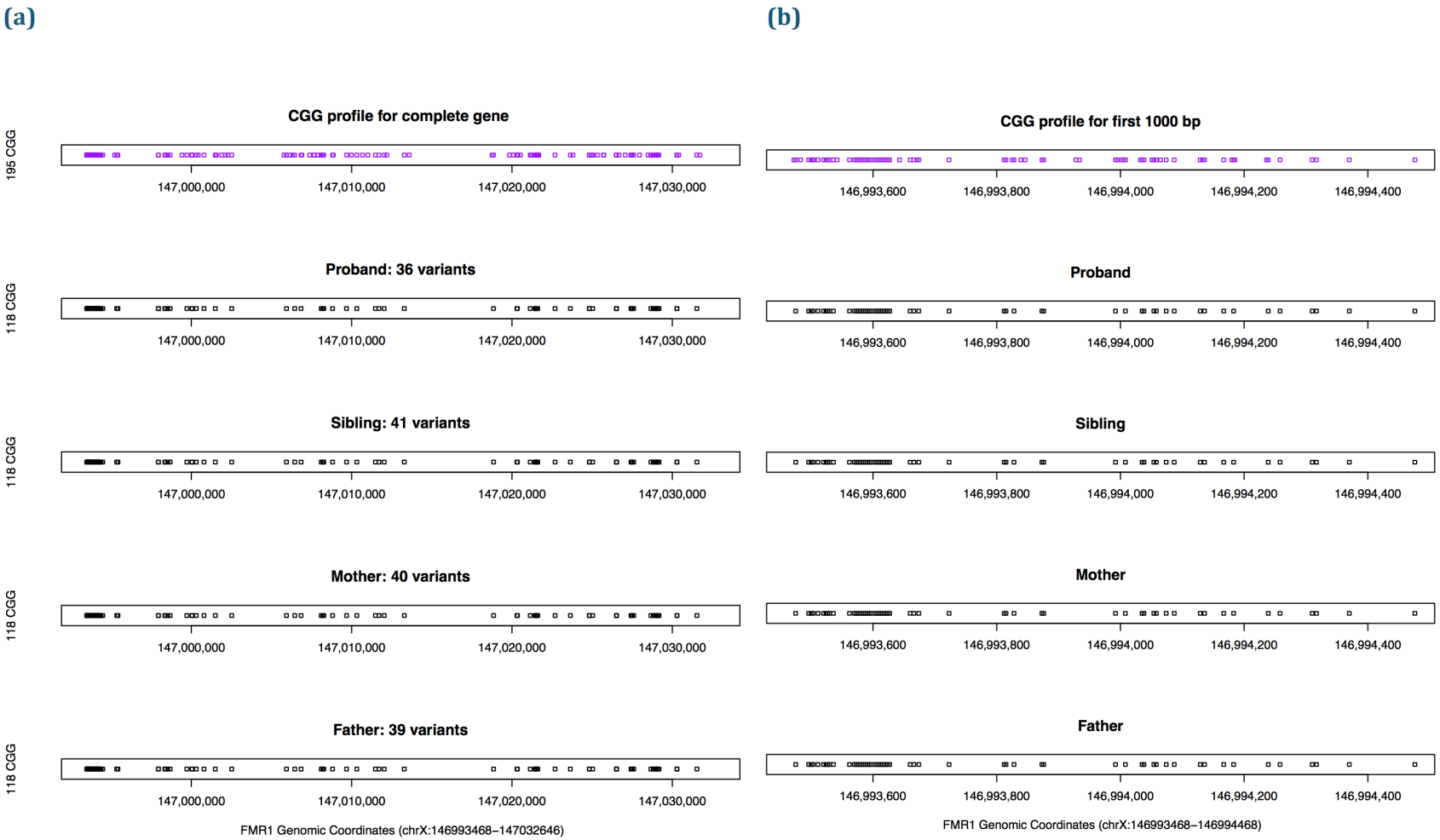

Supplemental Figure 6

(a)

(b)

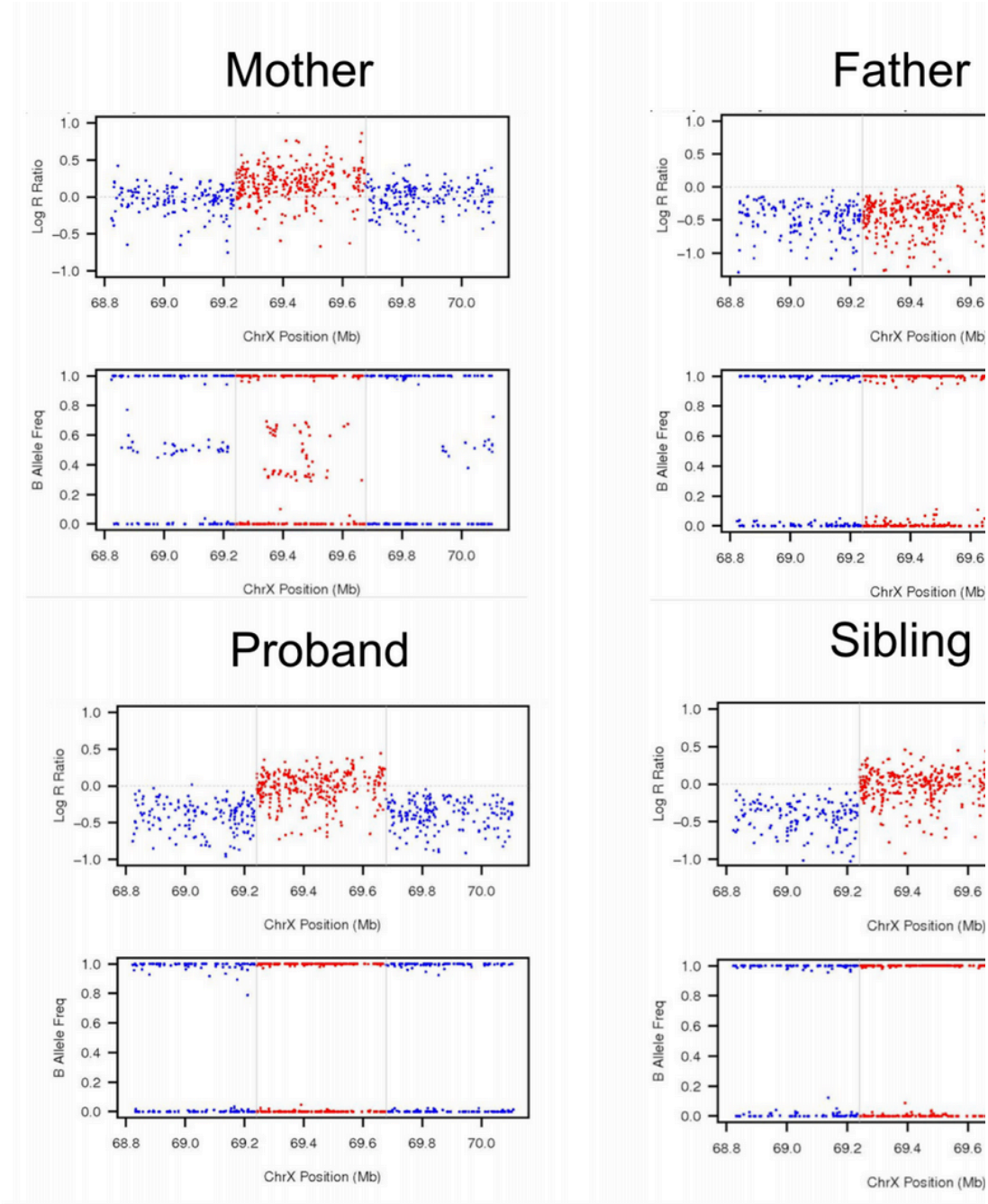

Supplemental Figure 7.

(a)

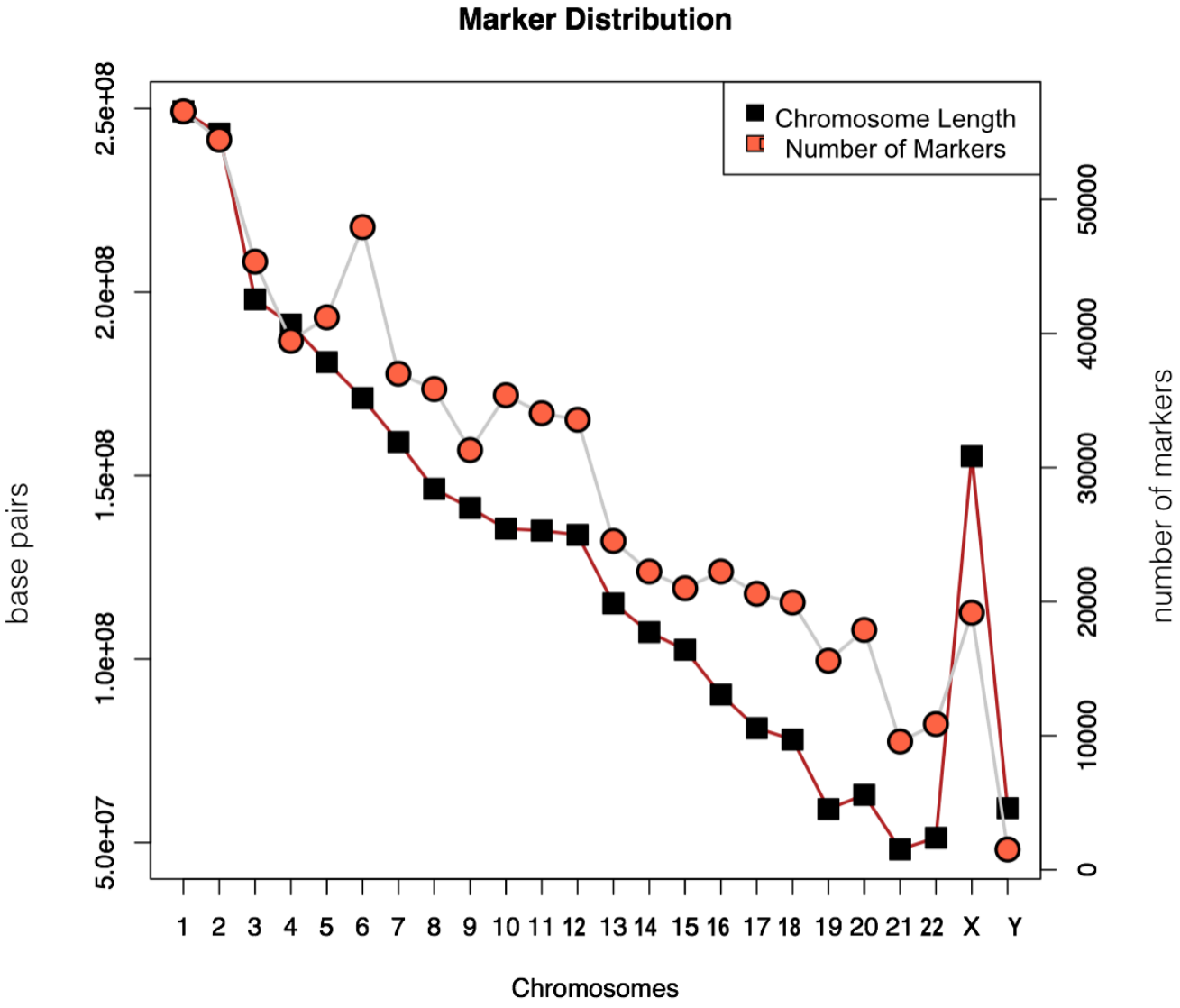

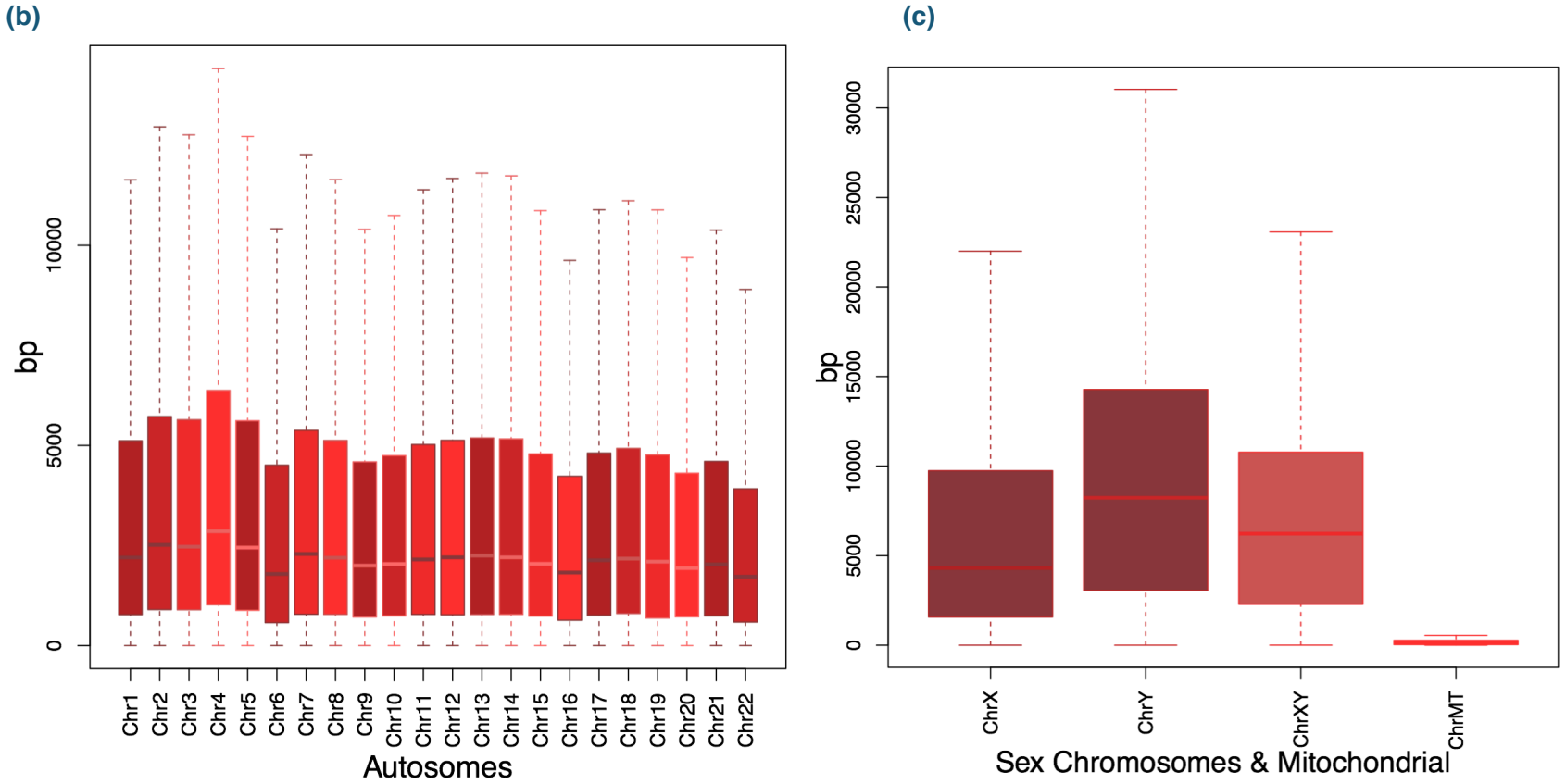
(b)
bp
0
5000
10000
Chr1
Chr2
Chr3
Chr4
Chr5
Chr6
Chr7
Chr8
Chr9
Chr10
Chr11
Chr12
Chr13
Chr14
Chr15
Chr16
Chr17
Chr18
Chr19
Chr20
Chr21
Chr22
Autosomes
(c)
bp
0
5000
10000
15000
20000
25000
30000
ChrX
ChrY
ChrXY
ChrMT
Sex Chromosomes & Mitochondrial

Supplemental Figure 8.

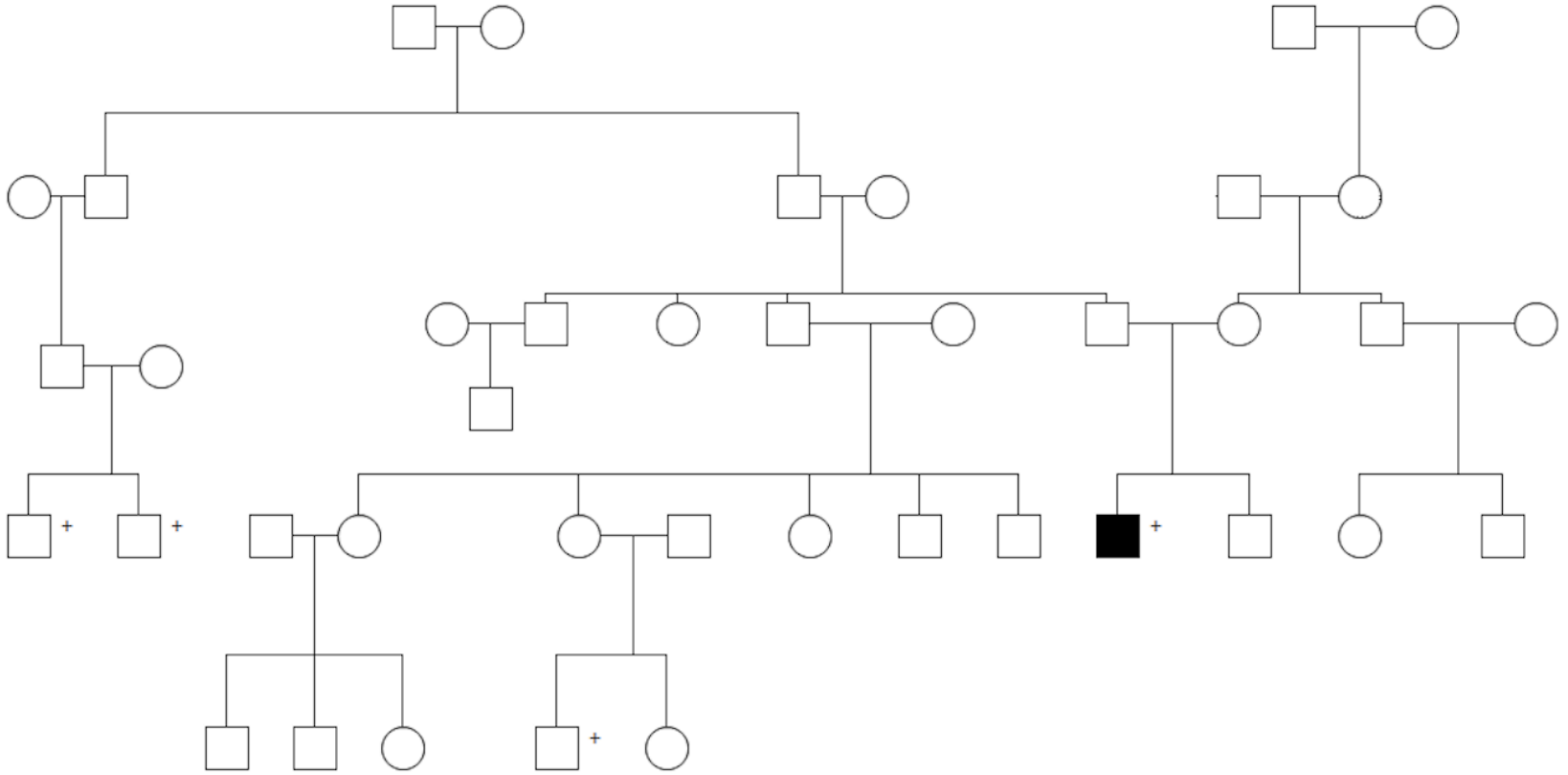

Supplemental Figure Legends

Supplemental Figure 1. MYBBP1A stop gain validation by Sanger sequencing. Sanger sequencing validation shows two overlapping peaks: one for C and one for T on the reverse strand.

Supplemental Figure 2. GGG repeats profile on the reference FMR1 complete gene and a simulated expansion. (a) The x axis represent the coordinates of the reference FMR1 gene, which includes the 5'UTR region where the CGG expansion occurs. **(b)** Here only the first 1000 closest nucleotides to the 5'UTR are plotted so a simulated expansion of randomly introduced CGG repeats is clearly appreciated.

Supplemental Figure 3. GGG repeats profile. Family K21 Complete FMR1 region profile. (a) The complete FMR1 gene CGG profile for this family looks normal, the number of CCG repeats for the proband is even less than the reference **(b)** First 1000 closest nucleotides to the 5'UTR.

Supplemental Figure 4. GGG repeats profile for family SSC_1. (a) The complete FMR1 gene CGG profile for this family looks normal. **(b)** The first 1000 closest nucleotides to the 5'UTR look normal.

Supplemental Figure 5. GGG repeats profile for family SSC_2. (a) The complete FMR1 gene CGG profile for this family also looks normal. **(b)** The first 1000 closest nucleotides to the 5'UTR look normal.

Supplemental Figure 6 (a). Copy number variation on K21 detected by CMA, Illumina Omni2.5 array and WGS technologies. Here is the duplication region that was previously reported on the medical records which reported the following genes fully contained in the CNV: OTUD6A/IGBP1/DGAT2L6/AWAT1/AWAT2/P2RY4/KIF4A/ARR3/GDPD2/RAB41/PDZD11 and the following genes partially contained in the CNV: EDA/DLG3/DLG3 which actually corresponds to the genes contained in the CNV region reported by ERDS. As the healthy male sibling also inherited. **(b)** Even though PennCNV did not detect the CNV, by plotting the LRR and BAF values for all the family, the CNV can be confirmed to be present in the mother, proband and healthy sibling.

Supp. Figure 7. Markers Number by chromosome and the inter-marker spacing. The recommended methods for filtering Copy Number Variants called from microarray data are too arbitrary in the sense they are not aware of some features array-specific that could make this general filtering criteria suitable for all microarray calls. The number of markers and the space between them was evaluated for each chromosome and considered into the CNVs filtering criteria. **(a)** Here, the size of the chromosomes in base pairs (black) and the number of markers (red) are plotted, a line is drown across the dots so it's easier to see that the greater the chromosome size, the greater the number of markers. However, the relation is not perfect and the number of markers for similar sized chromosomes, can vary largely. Because of this, the expected number of SNPs involved in a CNV call from one chromosome has to differ from those called in another chromosome. **(b)** However, not only the number of markers plays an important role but it was also important to make sure that the marker distribution across each chromosome was homogeneous without clusters of markers and large empty regions. If the size in base pairs of each chromosome was divided between the number of markers, the average inter-marker spacing should be 5Kb, to know if this was true, all the values for the spaces between markers (without outliers) are plotted here as quartiles, showing that 3/4 of the spacing

values are around 5 or 6Kb and the other quarter having inter-marker spaces up to 10Kb, which explains why some regions are more difficult to call. **(c)** The sex chromosomes are plotted separately as their upper quartile has greater values than the autosomes. In the other hand, the Mitochondrial chromosome inter-marker spacing is smaller, this make sense as it's size is only of ~16Kb and the Illumina Omni2.5 microarray has 288 markers for it.

Supp. Figure 8. Extended Pedigree K21. Individuals with a + sign are affected by ???. The black square represents the K21 proband analyzed in this study.

Family	Model	Chromosome	Start	End	Ref	Alt	CADD score
SSC_1	AutRec	chr18	56296796	56296801	CACACA	-	20.8
SSC_1	AutRec	chr1	22862796	22862796	T	C	22.4
SSC_1	AutRec	chr11	11228877	11228877	A	G	26.3
SSC_1	AutRec	chr20	37967464	37967464	C	G	25.7
SSC_1	DeNovo	chr1	219547206	219547207	AA	-	23.4
SSC_1	DeNovo	chr1	97159431	97159432	TT	-	21.6
SSC_1	DeNovo	chr11	79222737	79222737	-	ACACACAT	25.5
SSC_1	DeNovo	chr13	88766728	88766729	TC	-	20.8
SSC_1	DeNovo	chr2	121269539	121269539	A	-	20.3
SSC_1	DeNovo	chr7	145605410	145605410	A	-	21.4
SSC_1	DeNovo	chr1	83889368	83889368	C	T	23
SSC_1	DeNovo	chr14	97431801	97431801	A	T	21
SSC_1	DeNovo	chr16	73924770	73924770	A	C	20.4
SSC_1	DeNovo	chr17	25783776	25783776	G	A	21.1
SSC_1	DeNovo	chr2	174526700	174526700	A	T	24.9
SSC_1	DeNovo	chr3	18950958	18950958	G	A	21.4
SSC_1	DeNovo	chr3	88859609	88859609	C	A	22.5
SSC_1	DeNovo	chr5	121878403	121878403	A	T	20.9
SSC_1	DeNovo	chr5	163435978	163435978	C	A	20.5
SSC_1	DeNovo	chr5	170260699	170260699	C	T	20.3
SSC_1	DeNovo	chr6	57564457	57564457	T	G	20.1
SSC_1	DeNovo	chr8	106076378	106076378	T	G	21
SSC_1	DeNovo	chr9	112286567	112286567	A	T	21.3
SSC_1	DeNovo	chr9	132190884	132190884	C	T	20.5
SSC_1	DeNovo	chr9	27670625	27670625	A	G	29.3
SSC_1	X_Linked	chr11	115803295	115803300	CAATCA	T	24.9
SSC_1	X_Linked	chr2	153153402	153153488	ATGTTTCTCT(	-	23.8
SSC_1	X_Linked	chr5	91090315	91090316	CA	T	20.1
SSC_1	X_Linked	chr6	106357487	106357509	GTGCATGGC1	-	22
SSC_1	X_Linked	chr8	132824962	132824975	GTGTGTGTG1	-	21.7
SSC_1	X_Linked	chr1	88929834	88929834	A	T	23.3
SSC_1	X_Linked	chr10	58879722	58879722	A	G	24
SSC_1	X_Linked	chr10	60606856	60606856	T	A	23.9
SSC_1	X_Linked	chr10	63403543	63403543	C	A	20.5
SSC_1	X_Linked	chr10	71303491	71303491	A	G	23.7
SSC_1	X_Linked	chr11	124716092	124716092	C	T	26.2
SSC_1	X_Linked	chr11	15780647	15780647	G	A	20.3
SSC_1	X_Linked	chr11	15861794	15861794	G	T	20.9
SSC_1	X_Linked	chr11	81529166	81529166	A	G	24.8
SSC_1	X_Linked	chr12	127097187	127097187	T	C	22
SSC_1	X_Linked	chr13	112225526	112225526	C	T	27.5
SSC_1	X_Linked	chr14	25971418	25971418	A	G	24.4
SSC_1	X_Linked	chr14	28712495	28712495	C	G	23.8

SSC_1	X_Linked	chr14	57207364	57207364	T	C	23.2
SSC_1	X_Linked	chr14	59545027	59545027	G	A	21
SSC_1	X_Linked	chr14	83287826	83287826	T	C	21.3
SSC_1	X_Linked	chr14	83347284	83347284	T	A	23.4
SSC_1	X_Linked	chr15	57619867	57619867	A	G	29
SSC_1	X_Linked	chr15	62055088	62055088	G	T	20.1
SSC_1	X_Linked	chr15	72892707	72892707	G	A	22.9
SSC_1	X_Linked	chr17	14584777	14584777	G	T	20.7
SSC_1	X_Linked	chr18	45326973	45326973	G	A	20.2
SSC_1	X_Linked	chr18	67037686	67037686	G	C	20.9
SSC_1	X_Linked	chr2	122728041	122728041	A	G	25.3
SSC_1	X_Linked	chr2	126951391	126951391	T	C	24.6
SSC_1	X_Linked	chr2	138864352	138864352	T	C	23.7
SSC_1	X_Linked	chr2	147340830	147340830	A	T	24.5
SSC_1	X_Linked	chr2	148113998	148113998	C	T	25.5
SSC_1	X_Linked	chr2	156118240	156118240	A	G	22.7
SSC_1	X_Linked	chr2	2832756	2832756	G	A	21.4
SSC_1	X_Linked	chr20	11017899	11017899	G	A	25.4
SSC_1	X_Linked	chr20	5279049	5279049	T	C	26.6
SSC_1	X_Linked	chr20	5279051	5279051	T	C	27.4
SSC_1	X_Linked	chr3	190806183	190806183	G	T	25.6
SSC_1	X_Linked	chr3	65290074	65290074	T	C	23.7
SSC_1	X_Linked	chr4	112669550	112669550	T	C	32
SSC_1	X_Linked	chr4	112736297	112736297	T	G	22.6
SSC_1	X_Linked	chr4	118823288	118823288	T	C	21.8
SSC_1	X_Linked	chr4	130168145	130168145	T	C	28.4
SSC_1	X_Linked	chr4	130443766	130443766	G	A	24.8
SSC_1	X_Linked	chr4	147575215	147575215	T	G	22.5
SSC_1	X_Linked	chr4	149381748	149381748	A	C	21.3
SSC_1	X_Linked	chr4	169969161	169969161	A	C	20.4
SSC_1	X_Linked	chr4	17252272	17252272	C	T	22
SSC_1	X_Linked	chr4	18180348	18180348	G	A	21.9
SSC_1	X_Linked	chr4	22881303	22881303	T	C	27.6
SSC_1	X_Linked	chr4	67841685	67841685	T	C	21.5
SSC_1	X_Linked	chr5	124316013	124316013	G	C	22
SSC_1	X_Linked	chr5	30453417	30453417	A	G	20.5
SSC_1	X_Linked	chr5	86837724	86837724	A	G	21.3
SSC_1	X_Linked	chr5	86870158	86870158	G	A	21.9
SSC_1	X_Linked	chr5	87009307	87009307	C	T	21
SSC_1	X_Linked	chr5	87296764	87296764	C	T	25.3
SSC_1	X_Linked	chr5	87343056	87343056	A	C	22.7
SSC_1	X_Linked	chr5	94682116	94682116	A	C	26.1
SSC_1	X_Linked	chr6	122419624	122419624	C	T	21.2
SSC_1	X_Linked	chr6	143740082	143740082	A	G	28

SSC_1	X_Linked	chr6	148282813	148282813	G	T	25
SSC_1	X_Linked	chr6	40574804	40574804	C	T	29.2
SSC_1	X_Linked	chr6	67067895	67067895	T	C	25.6
SSC_1	X_Linked	chr7	14101770	14101770	C	T	21.4
SSC_1	X_Linked	chr7	155665998	155665998	T	G	20.2
SSC_1	X_Linked	chr7	156821142	156821142	G	A	28.4
SSC_1	X_Linked	chr8	122228750	122228750	G	T	20.1
SSC_1	X_Linked	chr8	124174622	124174622	C	G	20.6
SSC_1	X_Linked	chr8	23844495	23844495	G	A	23.4
SSC_1	X_Linked	chr8	37211547	37211547	G	A	28.7
SSC_1	X_Linked	chr8	37478445	37478445	G	A	23.3
SSC_1	X_Linked	chr8	64544103	64544103	G	A	25.4
SSC_1	X_Linked	chr8	82285517	82285517	C	T	25.4
SSC_1	X_Linked	chr9	116552467	116552467	C	G	34
SSC_1	X_Linked	chr9	118422612	118422612	G	A	21.7
K21	AutRec	chr22	27687672	27687672	C	T	20.4
K21	AutRec	chr3	61335581	61335581	A	C	25.4
K21	AutRec	chr3	61335633	61335633	G	C	20.1
K21	AutRec	chr5	123532440	123532440	G	T	24.1
K21	AutRec	chr5	9965489	9965489	C	T	21.1
K21	AutRec	chr6	50840399	50840399	A	G	21.9
K21	AutRec	chr7	41117784	41117784	T	C	28.4
K21	DeNovo	chr1	83856628	83856629	TG	-	22.4
K21	DeNovo	chr3	101042787	101042794	CACACACC	-	27.7
K21	DeNovo	chr5	56260260	56260260	-	T	21.8
K21	DeNovo	chr15	56076095	56076095	C	T	22.2
K21	DeNovo	chr20	20860914	20860914	G	A	21
K21	DeNovo	chr6	923029	923029	G	A	21.2
K21	DeNovo	chr9	132190774	132190774	T	C	27.2
K21	DeNovo	chr9	132190776	132190776	C	T	21.9
K21	DeNovo	chr9	132190777	132190777	G	A	25
K21	DeNovo	chrX	40247640	40247640	A	C	23
K21	X_Linked	chr15	56076080	56076091	ACACACACA(	-	20.1
K21	X_Linked	chr5	61072614	61072619	GGCTCC	-	20.2
K21	X_Linked	chr6	106357487	106357509	GTGCATGGC1	-	22
K21	X_Linked	chr6	106357512	106357540	TTTATTTGCA/	-	20.3
K21	X_Linked	chr1	4583312	4583312	G	A	24
K21	X_Linked	chr1	53871085	53871085	G	C	21.7
K21	X_Linked	chr1	73408392	73408392	G	A	21.5
K21	X_Linked	chr10	113688392	113688392	T	C	21.5
K21	X_Linked	chr11	133467379	133467379	C	A	21.5
K21	X_Linked	chr12	122086571	122086571	G	A	20.6
K21	X_Linked	chr13	40562721	40562721	G	A	23
K21	X_Linked	chr13	53586912	53586912	T	C	25.5

K21	X_Linked	chr13	53860192	53860192	A	G	23.7
K21	X_Linked	chr13	54739462	54739462	G	A	28.2
K21	X_Linked	chr14	101851050	101851050	G	A	20.8
K21	X_Linked	chr14	61096535	61096535	G	A	22.4
K21	X_Linked	chr14	98708466	98708466	C	A	21
K21	X_Linked	chr14	99090043	99090043	C	T	23
K21	X_Linked	chr15	36592921	36592921	T	C	26.8
K21	X_Linked	chr15	70690919	70690919	A	T	20.5
K21	X_Linked	chr18	19484595	19484595	A	G	29
K21	X_Linked	chr18	76008014	76008014	G	A	23.7
K21	X_Linked	chr19	32514015	32514015	T	C	31
K21	X_Linked	chr2	118464682	118464682	G	A	26.2
K21	X_Linked	chr2	191069238	191069238	T	C	22.7
K21	X_Linked	chr3	112693983	112693983	T	G	28.1
K21	X_Linked	chr3	118572351	118572351	C	T	23.8
K21	X_Linked	chr3	125705514	125705514	G	C	21.1
K21	X_Linked	chr3	160295077	160295077	C	T	23.8
K21	X_Linked	chr3	51702481	51702481	T	G	20.8
K21	X_Linked	chr4	14342075	14342075	T	C	21.4
K21	X_Linked	chr4	182824707	182824707	C	T	22.8
K21	X_Linked	chr4	19056340	19056340	C	T	21.9
K21	X_Linked	chr4	24378792	24378792	C	G	22.4
K21	X_Linked	chr4	26860116	26860116	G	A	23.9
K21	X_Linked	chr4	30374172	30374172	G	A	20.5
K21	X_Linked	chr5	103344498	103344498	C	A	22.1
K21	X_Linked	chr5	103553737	103553737	T	C	21
K21	X_Linked	chr5	107154028	107154028	T	C	21.4
K21	X_Linked	chr5	109260124	109260124	T	C	22.3
K21	X_Linked	chr5	114649524	114649524	G	A	21.8
K21	X_Linked	chr5	123276353	123276353	C	T	23.2
K21	X_Linked	chr5	166069017	166069017	C	T	20.9
K21	X_Linked	chr5	166587688	166587688	T	C	22.2
K21	X_Linked	chr5	171086955	171086955	C	G	26.9
K21	X_Linked	chr5	171712758	171712758	T	C	27.8
K21	X_Linked	chr5	3115792	3115792	G	T	32
K21	X_Linked	chr5	4778242	4778242	C	T	27
K21	X_Linked	chr5	50814113	50814113	C	T	34
K21	X_Linked	chr5	61035688	61035688	A	G	28.8
K21	X_Linked	chr5	73787644	73787644	T	A	22
K21	X_Linked	chr5	86942915	86942915	C	T	28.2
K21	X_Linked	chr5	92145245	92145245	A	C	21.9
K21	X_Linked	chr6	106957825	106957825	C	T	22.7
K21	X_Linked	chr6	22558596	22558596	A	G	23.3
K21	X_Linked	chr6	48060847	48060847	A	G	24.4

K21	X_Linked	chr6	57675003	57675003	A	G	21.1
K21	X_Linked	chr6	7631966	7631966	C	T	20.1
K21	X_Linked	chr6	77104723	77104723	G	A	20.4
K21	X_Linked	chr6	88688027	88688027	T	C	27.2
K21	X_Linked	chr7	41174953	41174953	A	G	25.6
K21	X_Linked	chr8	10427001	10427001	A	T	27.7
K21	X_Linked	chr8	135352051	135352051	G	T	21
K21	X_Linked	chr8	20248897	20248897	C	T	22.9
K21	X_Linked	chr8	21481008	21481008	C	T	24.5
K21	X_Linked	chr9	108671886	108671886	G	C	21.7
K21	X_Linked	chr9	108978316	108978316	C	T	21.4
K21	X_Linked	chr9	118745741	118745741	G	A	25.2
K21	X_Linked	chr9	29591346	29591346	A	C	21.2
K21	X_Linked	chr9	34719492	34719492	C	A	20.7
K21	X_Linked	chr9	36809058	36809058	A	G	22
SSC_2	AutRec	chr5	148861846	148861846	T	C	21.4
SSC_2	AutRec	chr5	166473408	166473408	A	G	32
SSC_2	AutRec	chr6	105392777	105392777	G	A	26.1
SSC_2	DeNovo	chr1	40157507	40157507	-	CCC	20.4
SSC_2	DeNovo	chr6	99633447	99633447	-	AA	26.1
SSC_2	DeNovo	chr7	41486661	41486661	A	-	20.2
SSC_2	DeNovo	chr8	97126161	97126186	GAGAGAGAG	-	25.7
SSC_2	DeNovo	chr8	97126173	97126186	GTGTGTGTGT	-	26.7
SSC_2	DeNovo	chr15	98525665	98525665	G	A	20
SSC_2	DeNovo	chr16	73798270	73798270	G	T	20.9
SSC_2	DeNovo	chr18	38192440	38192443	GACC	AACA	21.7
SSC_2	DeNovo	chr2	143423002	143423002	T	C	20.2
SSC_2	DeNovo	chr20	37967451	37967451	A	C	28.5
SSC_2	DeNovo	chr20	52894853	52894853	G	T	24.7
SSC_2	DeNovo	chr20	83275	83275	T	C	21.3
SSC_2	DeNovo	chr3	75913410	75913410	C	G	24.7
SSC_2	DeNovo	chr4	113424391	113424391	C	T	21.5
SSC_2	DeNovo	chr4	150225458	150225458	A	T	31
SSC_2	DeNovo	chr9	13447092	13447092	T	A	23.2
SSC_2	X_Linked	chr11	114130425	114130428	ACTC	G	23.2
SSC_2	X_Linked	chr16	54397489	54397489	-	AG	25.7
SSC_2	X_Linked	chr17	68625736	68625742	ACACACA	-	22.7
SSC_2	X_Linked	chr2	180748704	180748704	T	-	25.1
SSC_2	X_Linked	chr22	27954051	27954051	-	TGTGTGTGTG	20.5
SSC_2	X_Linked	chr3	16356392	16356396	TAAGA	-	21.9
SSC_2	X_Linked	chr5	152622997	152622997	-	CT	25.6
SSC_2	X_Linked	chr5	61050514	61050526	AGTCTAAGAT	-	21
SSC_2	X_Linked	chr8	78870672	78870673	AG	-	24.5
SSC_2	X_Linked	chr1	115944429	115944429	G	A	21.7

SSC_2	X_Linked	chr1	209515989	209515989	G	A	25.2
SSC_2	X_Linked	chr1	230059707	230059707	T	G	20.3
SSC_2	X_Linked	chr1	26492528	26492528	G	A	21.8
SSC_2	X_Linked	chr10	124858110	124858110	C	T	23
SSC_2	X_Linked	chr10	128395835	128395835	C	T	21.2
SSC_2	X_Linked	chr10	130983110	130983110	T	A	28.7
SSC_2	X_Linked	chr10	131121537	131121537	A	T	29.1
SSC_2	X_Linked	chr10	131191050	131191050	G	A	26.3
SSC_2	X_Linked	chr10	131215926	131215926	A	C	23.5
SSC_2	X_Linked	chr10	66344166	66344166	G	A	20.8
SSC_2	X_Linked	chr11	115390478	115390478	G	T	20.7
SSC_2	X_Linked	chr11	119663944	119663944	C	T	22.6
SSC_2	X_Linked	chr11	13255161	13255161	C	T	23
SSC_2	X_Linked	chr11	13846999	13846999	A	G	25.2
SSC_2	X_Linked	chr11	75940022	75940023	AA	CC	21.5
SSC_2	X_Linked	chr11	80129375	80129375	G	C	21.2
SSC_2	X_Linked	chr12	113886945	113886945	G	A	29.6
SSC_2	X_Linked	chr12	19562222	19562222	C	T	22.2
SSC_2	X_Linked	chr12	26281499	26281499	T	A	22.7
SSC_2	X_Linked	chr12	54699087	54699087	T	C	26
SSC_2	X_Linked	chr12	88842526	88842526	C	T	20.2
SSC_2	X_Linked	chr13	34578005	34578005	C	A	21.5
SSC_2	X_Linked	chr13	53991175	53991175	T	C	21.1
SSC_2	X_Linked	chr13	60050575	60050575	A	G	28
SSC_2	X_Linked	chr13	74802722	74802722	A	G	24.6
SSC_2	X_Linked	chr13	79580367	79580367	G	T	24.3
SSC_2	X_Linked	chr13	82081219	82081219	A	G	20.4
SSC_2	X_Linked	chr14	66339078	66339078	T	C	21.6
SSC_2	X_Linked	chr15	47341462	47341462	A	G	20.3
SSC_2	X_Linked	chr15	60055405	60055405	T	C	31
SSC_2	X_Linked	chr15	93833334	93833334	C	T	23
SSC_2	X_Linked	chr15	96548743	96548743	A	T	32
SSC_2	X_Linked	chr16	51026783	51026783	G	A	26.5
SSC_2	X_Linked	chr16	51279310	51279310	C	A	28.4
SSC_2	X_Linked	chr16	59033833	59033833	A	G	24
SSC_2	X_Linked	chr16	60300340	60300340	G	A	21.7
SSC_2	X_Linked	chr18	51628566	51628566	A	T	25.4
SSC_2	X_Linked	chr2	151619390	151619390	C	A	25.9
SSC_2	X_Linked	chr2	164331585	164331585	C	G	24
SSC_2	X_Linked	chr2	172957618	172957618	C	T	24.9
SSC_2	X_Linked	chr2	176130181	176130181	A	G	23.5
SSC_2	X_Linked	chr2	191069238	191069238	T	C	22.7
SSC_2	X_Linked	chr2	22153244	22153244	A	C	22.5
SSC_2	X_Linked	chr2	227559824	227559824	T	C	27.2

SSC_2	X_Linked	chr2	37975711	37975711	A	C	26.4
SSC_2	X_Linked	chr2	38001226	38001226	C	T	20.8
SSC_2	X_Linked	chr20	11020374	11020374	A	G	21.1
SSC_2	X_Linked	chr20	7306898	7306898	C	T	22.2
SSC_2	X_Linked	chr21	18115979	18115979	C	T	24.2
SSC_2	X_Linked	chr3	115056229	115056229	T	A	29.1
SSC_2	X_Linked	chr4	100608406	100608406	A	G	22.7
SSC_2	X_Linked	chr4	111125850	111125850	C	A	24.2
SSC_2	X_Linked	chr4	127008059	127008059	T	C	23.5
SSC_2	X_Linked	chr4	24378792	24378792	C	G	22.4
SSC_2	X_Linked	chr4	27726615	27726615	G	A	21.1
SSC_2	X_Linked	chr4	27759790	27759790	G	T	21.8
SSC_2	X_Linked	chr4	42222902	42222902	A	G	25.6
SSC_2	X_Linked	chr4	96756053	96756053	T	C	20.9
SSC_2	X_Linked	chr5	154973014	154973014	C	A	22.9
SSC_2	X_Linked	chr5	155113061	155113061	A	C	25.7
SSC_2	X_Linked	chr5	157541929	157541929	C	T	27.7
SSC_2	X_Linked	chr5	165337596	165337596	T	C	24.1
SSC_2	X_Linked	chr5	165525147	165525147	A	G	23.3
SSC_2	X_Linked	chr5	166028177	166028177	T	G	24.3
SSC_2	X_Linked	chr5	2848501	2848501	A	T	23.9
SSC_2	X_Linked	chr5	3187598	3187598	T	C	24.8
SSC_2	X_Linked	chr5	44441702	44441702	T	C	21.2
SSC_2	X_Linked	chr5	57367474	57367474	C	T	27.3
SSC_2	X_Linked	chr6	57731529	57731529	G	T	20.2
SSC_2	X_Linked	chr6	63165651	63165651	G	A	24.9
SSC_2	X_Linked	chr6	91956739	91956739	T	A	24
SSC_2	X_Linked	chr6	99606759	99606759	A	G	23.5
SSC_2	X_Linked	chr7	106684276	106684276	A	G	23.9
SSC_2	X_Linked	chr7	11357015	11357015	T	C	20.9
SSC_2	X_Linked	chr7	114990639	114990639	A	G	23.8
SSC_2	X_Linked	chr7	115340835	115340835	C	T	25.7
SSC_2	X_Linked	chr7	13842239	13842239	C	T	28
SSC_2	X_Linked	chr7	13866759	13866759	T	C	21.7
SSC_2	X_Linked	chr7	13874391	13874391	A	G	22.1
SSC_2	X_Linked	chr7	13879370	13879370	T	G	25.7
SSC_2	X_Linked	chr7	45499145	45499145	C	A	20.5
SSC_2	X_Linked	chr8	124297256	124297256	A	G	22.6
SSC_2	X_Linked	chr8	135046560	135046560	T	C	22.7
SSC_2	X_Linked	chr8	136342563	136342563	T	C	21.5
SSC_2	X_Linked	chr8	78361199	78361199	G	C	20.2
SSC_2	X_Linked	chr9	16278494	16278494	G	C	36
SSC_2	X_Linked	chr9	27763002	27763002	G	T	21.8
SSC_2	X_Linked	chr9	30243440	30243440	T	C	24.7

SSC_2	X_Linked	chr9	78473530	78473530	G	T	21.3
SSC_2	X_Linked	chr9	83995471	83995471	A	C	23
SSC_2	X_Linked	chrX	17351169	17351169	C	A	22.9
SSC_2	X_Linked	chrX	97109589	97109589	A	C	34